Molecular Genetics and Metabolism Reports 21 (2019) 100510

Contents lists available at ScienceDirect

Molecular Genetics and Metabolism Reports

journal homepage: www.elsevier.com/locate/ymgmr

# Intravenous delivery of a chemically modified sulfamidase efficiently reduces heparan sulfate storage and brain pathology in mucopolysaccharidosis IIIA mice

Susanne Gustavsson, Elisabet Ohlin Sjöström, Agneta Tjernberg, Juliette Janson, Ulrica Westermark, Tommy Andersson, Åsa Makower, Erik Arnelöf, Gudrun Andersson, Jan Svartengren, Carina Ekholm, Stefan Svensson Gelius*

*Research & Translational Science Unit, Swedish Orphan Biovitrum AB (publ), Stockholm, Sweden*

ARTICLE INFO

*Keywords:*
Mucopolysaccharidosis IIIA
Sanfilippo
Sulfamidase
Enzyme replacement therapy
Heparan sulfate
Neuroinflammation

ABSTRACT

Mucopolysaccharidosis type IIIA (MPS IIIA) is a lysosomal storage disorder (LSD) characterized by severe central nervous system (CNS) degeneration. The disease is caused by mutations in the *SGSH* gene coding for the lysosomal enzyme sulfamidase. Sulfamidase deficiency leads to accumulation of heparan sulfate (HS), which triggers aberrant cellular function, inflammation and eventually cell death. There is currently no available treatment against MPS IIIA. In the present study, a chemically modified recombinant human sulfamidase (CM-rhSulfamidase) with disrupted glycans showed reduced glycan receptor mediated endocytosis, indicating a non-receptor mediated uptake in MPS IIIA patient fibroblasts. Intracellular enzymatic activity and stability was not affected by chemical modification. After intravenous (i.v.) administration in mice, CM-rhSulfamidase showed a prolonged exposure in plasma and distributed to the brain, present both in vascular profiles and in brain parenchyma. Repeated weekly i.v. administration resulted in a dose- and time-dependent reduction of HS in CNS compartments in a mouse model of MPS IIIA. The reduction in HS was paralleled by improvements in lysosomal pathology and neuroinflammation. Behavioral deficits in the MPS IIIA mouse model were apparent in the domains of exploratory behavior, neuromuscular function, social- and learning abilities. CM-rhSulfamidase treatment improved activity in the open field test, endurance in the wire hanging test, sociability in the three-chamber test, whereas other test parameters trended towards improvements. The unique properties of CM-rhSulfamidase described here strongly support the normalization of clinical symptoms, and this candidate drug is therefore currently undergoing clinical studies evaluating safety and efficacy in patients with MPS IIIA.

## 1. Introduction

Mucopolysaccharidosis type IIIA (MPS IIIA), also known as Sanfilippo A, is an autosomal recessive lysosomal storage disease (LSD) caused by a functional deficiency in the *SGSH* gene. The *SGSH* gene codes for sulfamidase (EC 3.10.1.1), an N-sulfoglucosamine sulfohydrolase enzyme that catalyzes the hydrolysis of an N-linked sulfate group from the non-reducing terminal glucosamine residue of heparan sulfate (HS). Consequently, disease-causing mutations in the *SGSH* gene result in an insufficient degradation of HS and an accumulation of HS metabolites, *i.e.* sulfated oligosaccharides derived from the partial degradation of HS [45]. Although HS accumulates in lysosomes throughout the body, the disorder mainly affects the central nervous system (CNS) where it causes severe progressive degeneration. As a

*Abbreviations:* ADA, Anti-drug antibody; AF, Autofluorescence; BBB, Blood-brain barrier; CHO, Chinese hamster ovarian; CM-rhSulfamidase, Chemically modified recombinant human sulfamidase; CNS, Central nervous system; CPM, Chlorpheniramine maleate; ECL, Electrochemiluminescence; ERT, Recombinant enzyme replacement therapy; GFAP, Glial fibrillary acidic protein; HS, Heparan sulfate; LC-MS, Liquid chromatography-mass spectrometry; LC-MS/MS, Liquid chromatography-tandem mass spectrometry; LIMPII, Lysosomal integral membrane protein II; LSD, Lysosomal storage disease; M6P, Mannose 6-phosphate; MPS IIIA, Mucopolysaccharidosis type IIIA; MSD-ECL, Meso scale discovery electrochemiluminescence; MTX, Methotrexate; PBS, Phosphate buffered saline; PFA, Paraformaldehyde; PK, Pharmacokinetic; RT, Room temperature; SEC, Size exclusion chromatography; SEM, Standard error of mean; TFA, Trifluoroacetic acid; WT, Wild type

* Corresponding author at: Research & Translational Science Unit, Swedish Orphan Biovitrum AB (publ), SE-112 76 Stockholm, Sweden.
*E-mail address:* stefan.j.svenssongelius@sobi.com (S. Svensson Gelius).

https://doi.org/10.1016/j.ymgmr.2019.100510
Received 26 June 2019; Received in revised form 23 August 2019; Accepted 23 August 2019
Available online 07 September 2019

result, patients experience a wide range of symptoms, including developmental delay, increasing behavioral problems such as hyperactivity and an aggressive and destructive behavior, sleep disturbances, and a rapid decline in social and cognitive skills. Later in life, these behavioral symptoms diminish, but motor retardation emerges, and progressive dementia leads to withdrawal and developmental regression. Most patients die before the third decade of life [7,45]. It has been suggested that accumulated storage material may cause CNS pathology *via* neuroinflammation, inhibition of autophagy, and/or axonal dystrophy, but the mechanisms are not fully understood [1,3]. Currently there is no effective treatment for MPS IIIA, palliative care is the only option to date.

Primary MPS IIIA patient fibroblasts with a HS storage phenotype can be used to study uptake and potency of recombinant enzyme replacement therapy (ERT) drug candidates [29], whereas animal models of MPS IIIA can be used to test therapeutic strategies. A naturally occurring mouse model of sulfamidase deficiency has been described [4,5,9]. This MPS IIIA mouse model results from a spontaneous missense mutation (D31N) in the catalytic site of the sulfamidase enzyme that reduces its activity to ~3% of normal activity [4]. MPS IIIA mice exhibit many of the disease features of MPS IIIA in patients, including HS storage from birth, behavioral abnormalities from ~10 weeks of age that gradually worsen with age to include cognitive deficits from ~20 weeks of age [9,16,23]. Neuroinflammation, encompassing both astrogliosis and microgliosis, is a key component of the disease in MPS IIIA mice [32,47].

Reaching the target compartment in CNS is the major challenge for treating neuronopathic LSDs, and therapeutic strategies evaluated in the MPS IIIA mouse model have included recombinant ERT, direct gene transfer, and gene-modified autologous stem cell transplantation [16,34,6,18,38,40,48]. Sustained high serum concentrations of enzyme could potentially result in therapeutically meaningful levels in CNS. This theory is supported by studies on AAV8-mediated liver-directed gene therapy, where serum sulfamidase activity 5-fold higher than in wild type (WT) mice resulted in 50% reduction of storage material in brain of MPS IIIA mice [49]. Furthermore, preclinical studies in different LSD disease models indicate that partial reduction (~10 to 20%) of storage material in brain can be achieved by systemic administration of high doses over long time intervals [10,33,50]. Upon systemic administration, sulfamidase is rapidly cleared from circulation *via* the mannose 6-phosphate (M6P) receptor expressed in peripheral tissues. M6P-mediated transport across the blood brain barrier (BBB) is however limited to the first weeks of life in mice, and subsequently down-regulated by 8 weeks [43].

The present work explores the *in vitro* and *in vivo* properties of a modified recombinant human sulfamidase (CM-rhSulfamidase) subjected to a mild chemical procedure that partially disrupts glycan structures but preserves catalytic activity. By avoiding the M6P receptor interaction with CM-rhSulfamidase, the expected prolonged systemic exposure is assumed to facilitate distribution of CM-rhSulfamidase to the CNS. CM-rhSulfamidase endocytosis, potency and clearance were evaluated *in vitro* in primary MPS IIIA patient fibroblasts. Systemic exposure and presence of CM-rhSulfamidase in the CNS after intravenous (i.v.) administration was assessed in mice, and therapeutic efficacy of CM-rhSulfamidase in the CNS was explored in the MPS IIIA mouse model.

## 2. Methods

### 2.1. rhSulfamidase cloning, expression, purification, and modification

A stable Chinese hamster ovarian (CHO) cell line was generated by transducing cells with a plasmid with full length human sulfamidase cDNA under the control of a CMV promoter. Human sulfamidase was produced in a fed batch process and purified to apparent homogeneity using conventional ion exchange chromatography steps. Sulfamidase was further oxidized by incubation with sodium meta-periodate, followed by ethylene glycol quenching and subsequent sodium borohydride reduction. Incubation times concentrations and temperatures were optimized based on product appearance on SDS-PAGE, Size exclusion chromatography (SEC), glycan structure and enzymatic activity with the aim to obtain an active homogenous product. The final procedure involved oxidation with 15 mM sodium meta-periodate at 0 °C in the dark for 60 min in a phosphate buffer (pH 6.0), glycan oxidation quenching by addition of ethylene glycol to a final concentration of 192 mM for 15 min at 6 °C before sodium borohydride addition to the reaction mixture at a final concentration of 38 mM without prior buffer exchange. After incubation at 0 °C for 120 min in the dark, the resulting sulfamidase preparation was ultrafiltrated against 20 mM sodium phosphate, 100 mM NaCl, pH 6.0.

### 2.2. CM-rhSulfamidase and rhSulfamidase tryptic digestion for glycopeptide analyses

Prior to liquid chromatography-mass spectrometry (LC-MS) analysis, the protein (~10 μg) was reduced, alkylated and digested with trypsin. Reduction of the lyophilized protein was done by incubation in 5 μL DL-dithiothreitol (10 mM in 50 mM $NH_4HCO_3$) at 70 °C for 1 h. Subsequent alkylation with 5 μL iodoacetamide (55 mM in 50 mM $NH_4HCO_3$) was performed at room temperature (RT) and in the dark for 45 min. For tryptic digestion 30 μL 50 mM $NH_4HCO_3$, 5 mM $CaCl_2$, pH 8, and trypsin (0.2 μg/μL in 1% acetic acid) was added to a trypsin: protein ratio of 1:20 (*w*/w). Digestion was performed over-night at 37 °C. The digestion was quenched by adding trifluoroacetic acid (TFA) to a final concentration of 0.5%. Prior to analysis 50 μL 5% acetonitrile, 0.1% propionic acid and 0.02% TFA were added.

LC separation was performed by a Luna C18 column, 3.2 μ, 100 Å (100 × 2.1 mm). The column temperature was 40 °C, mobile phase A consisted of 5% acetonitrile, 0.1% propionic acid and 0.02% TFA, and mobile phase B consisted of 95% acetonitrile, 0.1% propionic acid and 0.02% TFA. The gradient used was 0–5 min: 0–10% B, 5–30 min: 10–70% B, 30–35 min: 70–90% B, 35.1 min: 0% B. A flow rate of 0.2 mL/min was used and the injection volume was 10–15 μL.

For the LC-MS analysis an Agilent 1200 HPLC system coupled to an Agilent 6510 Q-TOF-MS operated in positive electrospray ionization mode was used. The LC-MS system was controlled by a MassHunter Workstation. During the course of data acquisition, the fragmentor voltage, skimmer voltage, and octapole RF were set to 90, 65, and 750 V, respectively. For the LC-MS analyses, scan range was set between 300 and 2800 *m/z*. For the MS/MS analyses, Argon was used as collision gas, the collision energies were set to 10, 15, and 20 V, scan range 100–1800 *m/z*, and scan speed 1 scan/s.

### 2.3. Bioanalysis

Concentrations of CM-rhSulfamidase and rhSulfamidase and presence of antibodies against CM-rhSulfamidase, *i.e.* anti-drug antibodies (ADA), in serum, were determined by Meso Scale Discovery electrochemiluminescence (MSD-ECL) based bridging format immunoassays on MSD Multi-array streptavidin coated plates. Washing between incubations was performed twice with PBS-Tween. All incubations in RT were made on a plate shaker at 500 rpm. For CM-rhSulfamidase and rhSulfamidase, streptavidin coated plates were blocked (5% MSD Blocker A in PBS) and incubated for > 60 min at RT. After washing, sample dilutions (25 μL; standard, control and unknowns) and conjugate Master-mix reagent solution (25 μL) containing biotinylated rhSulfamidase specific monoclonal antibodies and ruthenium labeled polyclonal rabbit anti-rhSulfamidase antibodies (details on antibodies, see supplementary Table 2), were added and the plates were incubated for 60 min at RT.

To detect ADA, serum samples were diluted 1:4 with PBS-Tween and sample dilutions (25 μL) were pre-incubated with 50 μL mixed

conjugates (CM-rhSulfamidase-biotin and CM-rhSulfamidase-Sulfo-Rutag conjugates at equimolar concentrations) at 4–8 °C overnight on polypropylene plates. Streptavidin coated MSD plates were blocked (5% MSD Blocker A in PBS) either in parallel with the pre-incubation plates or for 60 min at RT. After washing, solutions from the pre-incubation plates (50 µL) were transferred to the streptavidin coated plates and incubated for 60 min (RT). Plates from both immuno assays were read on an MSD 1300 MESO QuickPlex SQ120 instrument after final washes with PBS-Tween and addition of Read buffer (diluted 1:1 with Milli-Q water; 150 µL/well).

For determination of HS levels in brain, liver, spleen, and cerebrospinal fluid (CSF), two liquid chromatography-tandem mass spectrometry (LC-MS/MS) methods were developed, one quantitative and one relative [26]. The quantitative method measures individual disaccharides derived from heparinase digestion of HS. Four HS digestion disaccharide products were included and the average concentration of the four disaccharides were set to be the reported HS level. The relative method monitors relative levels of sulfated HS metabolites, *i.e.* the tetrasaccharide GlcNS-UA-GlcNAc-UA (+1S), used as a marker for lysosomal storage of HS. The relative method was also used for the determination of the HS metabolite GlcNS-UA in human fibroblast cells.

### 2.4. In vitro based cellular experiments

For the *in vitro* based cellular experiments, a primary fibroblast cell line from a female MPS IIIA patient was used (GM00879, Coriell Institute). The cells were cultured according to the manufacturer's instructions and seeded at 1E + 04 cells/well in 96-well plates (1E + 04 cells/cm$^2$) or 1.5E + 05 cells/well in 6-well plates (1.6E + 04 cells/cm$^2$) with a viability of > 95%. All cells were incubated in a humidified incubator at 37 °C, 5% $CO_2$. After incubation, cells were harvested by washing twice with PBS followed by cell lysis directly in the plate using RIPA buffer supplemented with protease and phosphatase inhibitors (Thermo Fisher Scientific) for 15 min in RT. Intracellular rhSulfamidase and CM-rhSulfamidase content was analyzed by the immunoassay method described in 2.3.

To study the contribution of M6P receptor-mediated endocytosis, the cells were treated with either rhSulfamidase (0.1 µg/mL) or CM-rhSulfamidase (1 µg/mL) together with increasing concentrations of M6P (Sigma Aldrich) ranging from 0 to 2.5 mM.

For time dependent endocytosis experiments, test items were pre-diluted in growth medium at a concentration range from 0.05 µg/mL to 0.006 µg/mL for rhSulfamidase and from 5 µg/mL to 0.6 µg/mL for CM-rhSulfamidase in order to reach comparable intracellular concentrations of the test items at the first time-point. For dose dependent endocytosis experiments, test items were pre-diluted in growth medium at a concentration range from 5 µg/mL to 0.005 µg/mL before added to cells. The cells were incubated for 24 h.

To study the intracellular retention, test items were pre-diluted in growth medium at 0.05 µg/mL for rhSulfamidase and 2.5 µg/mL for CM-rhSulfamidase to reach comparable intracellular levels. Cells were incubated for 24 h followed by washing in PBS, after which fresh medium without the test items was added. For the “Day 0” time point, the plate was incubated in fresh medium for 5 h after treatment start, whereas the other plates were harvested, as described above, one per day, up to six days after the 24-h incubation with the test items.

To study intracellular activity, test items were pre-diluted in growth medium at a concentration range from 0.005 µg/mL to 0.0002 µg/mL for rhSulfamidase and 1.5 µg/mL to 0.05 µg/mL for CM-rhSulfamidase before addition to cells. Concentrations of test items were adjusted to reach comparable intracellular levels at a range where a concentration dependent consumption of HS could be detected. The cells were incubated for 24 h. After incubation, cells were washed once with PBS followed by trypsination to detach the cells, which were re-suspended in growth media, transferred to 1.5 mL tubes followed by centrifugation. The pellets were washed once with PBS followed by cell lysis by freeze/thaw cycles in 29 mM diethylbarbituric acid, 29 mM sodium acetate and 0.68% *w/v* sodium chloride, pH 6.5 supplemented with protease and phosphatase inhibitors. Cell debris was removed by centrifugation and the samples were divided into two aliquots, one for HS analysis by LC-MS/MS using the disaccharide biomarker GlcNS-UA [26] and one for rhSulfamidase/CM-rhSulfamidase content analysis.

### 2.5. In vivo experiments

Studies using mice were reviewed and approved by animal ethics committees and all procedures complied with regulations and recommendations. Efficacy and distribution studies were carried out at an AAALAC accredited facility and mice were maintained according to the animal welfare regulations of the Ministry of Science of the Austrian government.

#### 2.5.1. Pharmacokinetics

To study the impact of chemical modification on the pharmacokinetic (PK) profile, CM-rhSulfamidase or rhSulfamidase were dosed as a single 12 mg/kg i.v. administration *via* the lateral tail vein to male C57BL/6 J mice (Taconic-Europe A/S). From each mouse, three blood samples were drawn through the sublingual plexus with the terminal sample under anesthesia. A total of 12 mice were included in the study, six per test item. Sampling time points were 5 and 30 min, 1, 3, 7 and 24 h post-dose, with three samples per time point. From these blood samples collected into EDTA vials, plasma was prepared by centrifugation at 1270 *g* at 4 °C for 10 min. Samples were stored at ≤ −70 °C. Plasma clearance was obtained by subjecting concentration *versus* time data to Non-Compartmental Analysis (NCA) using Phoenix 64 WinNonlin version 7.0 NMLE (Phoenix, Pharsight Corp., USA). Values below the lower limit of quantification (LLOQ) were not included in the analysis.

#### 2.5.2. Pharmacodynamics

Male congenic C57BL/6 J mice carrying an inactivating spontaneous mutation in the *Sgsh* gene [4,5] and their unaffected male WT littermates were obtained from The Jackson Laboratory (B6.Cg-*Sgsh*$^{mps3a}$ JAX stock #003780). Animals were housed individually in individually ventilated cages on standard rodent bedding under a 12-h light-dark cycle. The room temperature was maintained at ~24 °C and standard rodent chow and water was available *ad libitum*. The health status of each individual animal was evaluated before study initiation and notable observations were recorded during the study. Randomization, allocation concealment, and blinding were used during the studies. Group allocation and number of animals in each group are specified in supplementary Table 1. All doses of CM-rhSulfamidase in the efficacy studies were given as enzymatically active doses. Four efficacy studies were performed, study A-D, a time-line diagram illustrating how the efficacy studies were carried out is presented in Fig. 1.

Groups of 9- to 11-week-old male MPS IIIA mice received i.v. injections of vehicle (50 mM arginine, 75 mM sodium chloride, 20 mg/mL sucrose at pH 7.8) or CM-rhSulfamidase at 3 to 22 mg/kg once weekly for 10, 20 or 25 weeks (supplementary Table 1). Mice received chlorpheniramine maleate (CPM) at 2.5 mg/kg subcutaneously 30 min prior to each i.v. injection to prevent hypersensitivity reactions. In addition, methotrexate (MTX) pre-treatments were used in two out of four efficacy studies to reduce anti-drug antibody (ADA) responses (Fig. 1). In Study B, MTX at 5 mg/kg was given one week before the first injection of vehicle or CM-rhSulfamidase, and again three days later, followed by repeated administrations of MTX 30 min prior to, as well as 24 and 48 h post, the first three weekly injections of vehicle or CM-rhSulfamidase. In Study D, groups or vehicle- and CM-rhSulfamidase-treated mice only received MTX at 5 mg/kg intraperitoneally at the first three weekly injections of vehicle or CM-rhSulfamidase as described above. Groups of naïve MPS IIIA and WT mice were included as negative controls in all studies. Body weights were recorded once a week. Groups of 27- to 34-

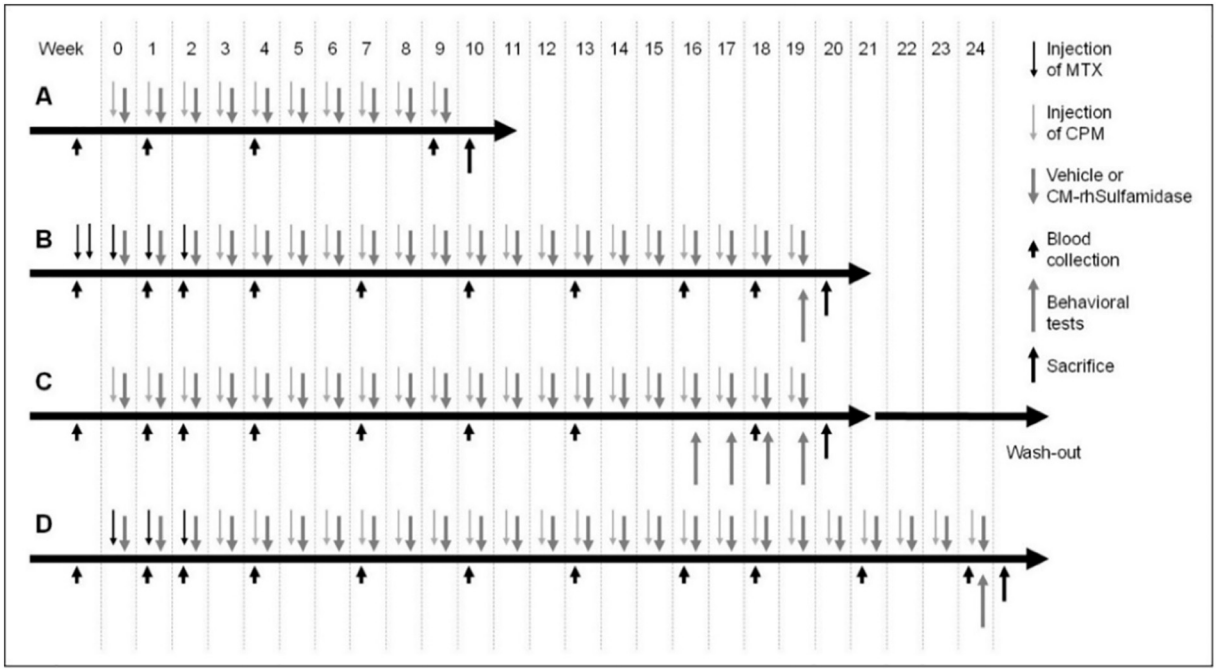


**Fig. 1.** Time-line diagrams to illustrate how the four efficacy studies (A to D) were carried out.

week-old male MPS IIIA mice and WT controls were exploratively evaluated for behavioral abnormalities and efficacy of CM-rhSulfamidase treatment by using a wire hanging test to assess neuromuscular function, an open field test to assess exploratory activity, a three-chamber social interaction test to assess social ability, and a Barnes maze test to assess learning ability and short-term memory. The different behavioral tests were only performed once or twice, using 8 to 16 individuals in each experimental group. For details on behavioral methods, see *Supplementary Methods*.

Blood samples were collected by mandibular bleeding from the facial vein/artery *plexus* one week prior to the first injection of CM-rhSulfamidase, and with regular intervals during the course of the studies (Fig. 1). Blood samples were allowed to clot at RT prior to centrifugation at 1000 $\times g$ for 10 min. Serum was harvested and stored frozen $\leq -70\,^{\circ}C$ until use. Unless otherwise stated, all mice were deeply anesthetized with an overdose of pentobarbital at 600 mg/kg intraperitoneally 24 h after the final injection of vehicle or CM-rhSulfamidase. CSF was obtained by dissection of muscles and exposure of *foramen magnum* followed by insertion of a Pasteur pipette into *cisterna magna*. Mice were placed in dorsal position, the thorax was opened, and blood was withdrawn from the right cardiac ventricle. After blood sampling, mice were transcardially perfused with physiological saline (0.9%) and brains were dissected and hemisected. Left hemispheres were frozen on dry ice for biochemical analyses, whereas right hemispheres were fixed by immersion in 4% paraformaldehyde in PBS as described below. Livers were also dissected, left liver lobes were frozen on dry ice, and the rest of the livers were fixed by immersion in 4% PFA. All frozen samples were stored $\leq -70\,^{\circ}C$ until use. Distribution to brain was explored in Study B by determining CM-rhSulfamidase concentration in brain homogenate of samples frozen for biochemical analysis at 24 h after the last of 20 weekly i.v. doses. The brain:serum ratio was calculated by dividing the concentration obtained in brain homogenate by the concentration in the serum sample obtained at termination with the assumption that 1 kg of brain tissue corresponded to 1 L.

### 2.5.3. Immunohistological processing and analyses

Analyses of central markers of efficacy and immunohistological localization of sulfamidase/CM-rhSulfamidase in brain were performed on material from three studies (A, C and D; Fig. 1). Brain sections from Study A (CM-rhSulfamidase at 6 and 18 mg/kg for 10 weeks) were analyzed for presence of sulfamidase as well as markers of lysosomal swelling (autofluorescent inclusions and lysosomal membrane protein, LIMP-2). Neuroinflammation (astrogliosis and microgliosis) was quantitatively analyzed in all three studies, data shown herein from Study D (CM-rhSulfamidase at 7 mg/kg for 25 weeks). Saline-perfused brains from Study A and D were hemisected and immersed in 4% PFA (in PBS pH 7.4) for one hour, transferred to 15% sucrose (in PBS) for cryoprotection for 24 h, and subsequently embedded in optimal cutting temperature (OCT) medium, frozen on dry ice and stored at $< -70\,^{\circ}C$. Cryosectioning was performed sagittally on a Leica CM 1950 cryotome at 10 µm thickness through five medio-lateral levels with 300 µm interdistance, starting at 0.24 mm lateral from the midline. Five sections per level were collected and intermediate sections were discarded. Five sections per animal (one section per level) were processed and analyzed for each immunohistochemical marker. Brains from Study C were processed for paraffin-embedding, hence fixed in 4% PFA for 24 h, dehydrated and embedded in paraffin. Paraffin-sectioning was done at 5 µm thickness on a slide microtome (Leica SM2000R). Representative levels were sampled in analogy to that described above, starting at 0.2 mm from the midline.

Immunohistochemistry procedures are described below. For a complete list of primary and secondary antibodies see supplementary Table 2. Sections were air-dried for 45 min followed by permeabilization in 0.3 or 1% Triton-X 100 in PBS. For chromogenic detection, endogenous peroxidases were quenched with hydrogen peroxidase in PBS for 30 min. Detection of lysosomes was preceded by an antigen retrieval step with 10% citrate at 95 °C for 15 min. Unspecific binding was blocked with 10% serum (goat or donkey) in PBS for 1 h. Primary antibody incubations were performed in blocking buffer. Three rinses with PBS were made between each step except between blocking and primary incubation (no rinse). Primary and secondary antibodies were incubated for 1 h and nuclear staining with DAPI for 10 min. To detect sulfamidase (and equally the test item CM-rhSulfamidase) in brain, a polyclonal affinity-purified antibody mixture raised in rabbit against CM-rhSulfamidase (pAb-3783) was used. Chromogenic staining was used to label microglia and astrocytes while fluorescence protocols were used to detect lysosomal membranes (LIMPII) and Sulfamidase/

CM-rhSulfamidase. Chromogenic development was achieved with ABC Elite kit followed by a DAB substrate kit (Vector Laboratories), according to manufacturer's instructions. Paraffin-embedded sections were counterstained with Harri's hematoxylin (Dako, S3309), dehydrated and coverslipped with Eukitt (Fluka, 03989). Selected regions of the brain, namely the cerebral cortex, hippocampus and cerebellum, were used for systematic quantitative image analysis. For image acquisition and quantitative image analysis details, see *Supplementary Methods*.

#### 2.5.4. Statistical analysis

Statistical analysis of data from pharmacodynamic studies was performed using GraphPad Prism 7.03 for Windows. Mean group values and the standard error of the mean (SEM) were reported. Parametric one-way ANOVA followed by Dunnett's multiple comparisons test *versus* one control group (vehicle) was applied for comparison between groups. If variances were found significantly different with $p < .05$ using Brown-Forsythe's test, non-parametric Kruskal-Wallis followed by Dunn's multiple comparisons test was applied. A two-way ANOVA for repeated measures with treatment and time factors, followed by Dunnett's multiple comparisons test, was performed for latency to reach target in the Barnes maze test. Grubb's outlier analysis was performed on selected datasets. Significance was set at $p < .05$ and was indicated by asterisks in the figures: $*p < .05$, $**p < .01$, $***p < .001$, and $****p < .0001$.

## 3. Results

### 3.1. Structural characteristics of CM-rhSulfamidase

Recombinant human sulfamidase was produced in a CHO cell line and purified to apparent homogeneity by a combination of several chromatography and filtration steps. The N-glycans at asparagines in position 21, 131, 244, and 393 were chemically modified *in vitro* by periodate oxidation followed by borohydride reduction. This procedure resulted in opening of glycan hexose rings by breaking the carbon carbon bond between cis-diol carbonyls. < 5% intact glycans remained after the procedure. Protocolls where more extensive oxidation and reduction steps were applied, resulted in a heterogenous product as judged from SDS-PAGE and SEC analysis (Data not shown). In Fig. 2A, an example of predicted bond breaks on mannose after chemical modification is shown. Detailed characterization of the modified glycan profile after chemical modification of CM-rhSulfamidase were performed using tryptic digestion followed by LC-MS analysis. Ions corresponding to the resulting chemically modified glycopeptides were detected and showed expected bond breaking. Fig. 2B shows an example of the T13 tryptic peptide NITR, containing Man-6 glycan, prior to and after chemical modification. The outcome of the chemical modification was considered reproducible as three batches of CM-rhSulfamidase modified with the same chemical modification protocol showed comparable bond breaks.

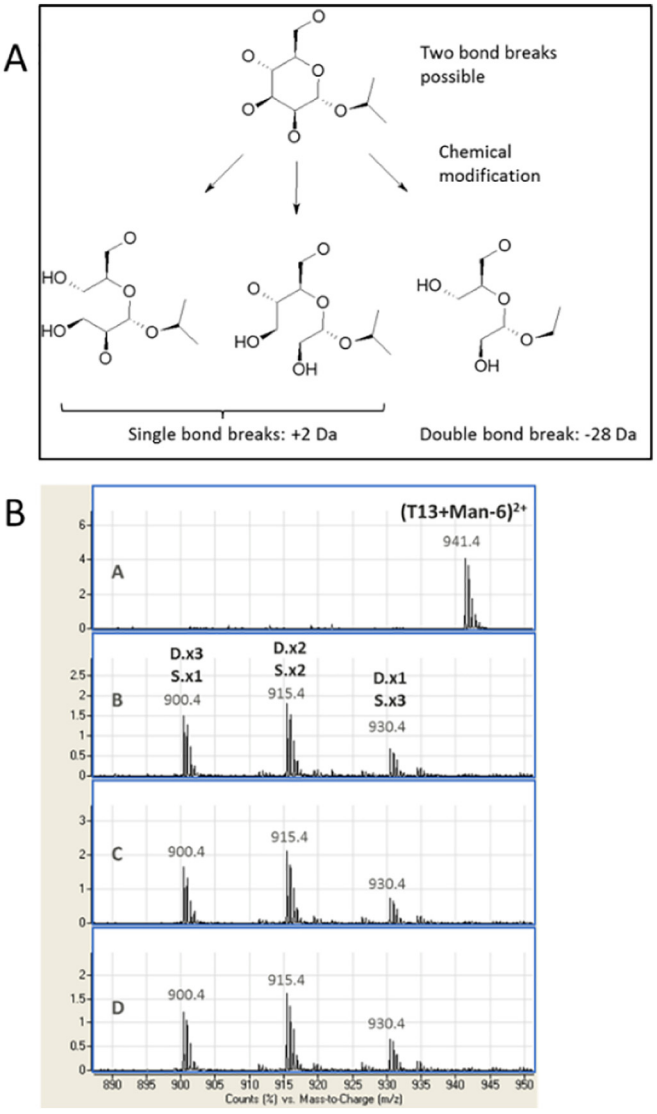


**Fig. 2.** Structural characteristics of chemically modified glycans of CM-rhSulfamidase (A) Example of predicted bond breaks on mannose after periodate oxidation and borohydride reduction. (B) Mass spectra prior and after chemical modification. Mass spectra of doubly charged ion(s) corresponding to tryptic peptide T13, NITR, with Man-6 glycan attached to N131. S = Single bond break; D = double (two) bond breaks, *e.g.* S. × 3 = 3 single bond breaks. A: Prior to chemical modification. B, C, D: After chemical modification of three batches of CM-rhSulfamidase.

### 3.2. Endocytosis of CM-rhSulfamidase by a non-receptor mediated process in MPS IIIA patient fibroblasts

To evaluate the effect of chemical modification on endocytosis, MPS IIIA fibroblasts were incubated with either CM-rhSulfamidase or rhSulfamidase. Endocytosis of CM-rhSulfamidase was significantly reduced compared to rhSulfamidase. In the concentration range studied, the rate of endocytosis was constant over a 24-hour period for both CM-rhSulfamidase and rhSulfamidase (data not shown), thus a 24-hour incubation time was applied throughout subsequent studies. To evaluate the concentration dependency of endocytosis, MPS IIIA patient fibroblasts were incubated with a concentration range from 0.1–5 μg/mL of either CM-rhSulfamidase or rhSulfamidase (Fig. 3A). Rate of endocytosis of CM-rhSulfamidase was directly proportional to its concentration in medium, indicative of a predominantly non-receptor mediated endocytosis process. In contrast, the endocytosis of rhSulfamidase was subjected to saturation in accordance with a receptor mediated process. A hyperbolic function could be fitted to rhSulfamidase data with a half-saturation constant of 1 μg/mL. Addition of M6P to the medium inhibited endocytosis of rhSulfamidase in a concentration dependent manner, indicating that endocytosis was predominantly mediated by the M6P receptor in these cells. M6P had no impact on endocytosis of CM-rhSulfamidase (Fig. 3B). Thus, the applied chemical modification strongly reduced glycan mediated endocytosis and pointed to non-receptor mediated endocytosis as the major endocytotic process for CM-rhSulfamidase in fibroblast cells.

### 3.3. Activity and long cellular retention of CM-rhSulfamidase in MPS IIIA patient fibroblasts

Next, any effect of CM-rhSulfamidase on the accumulation of HS

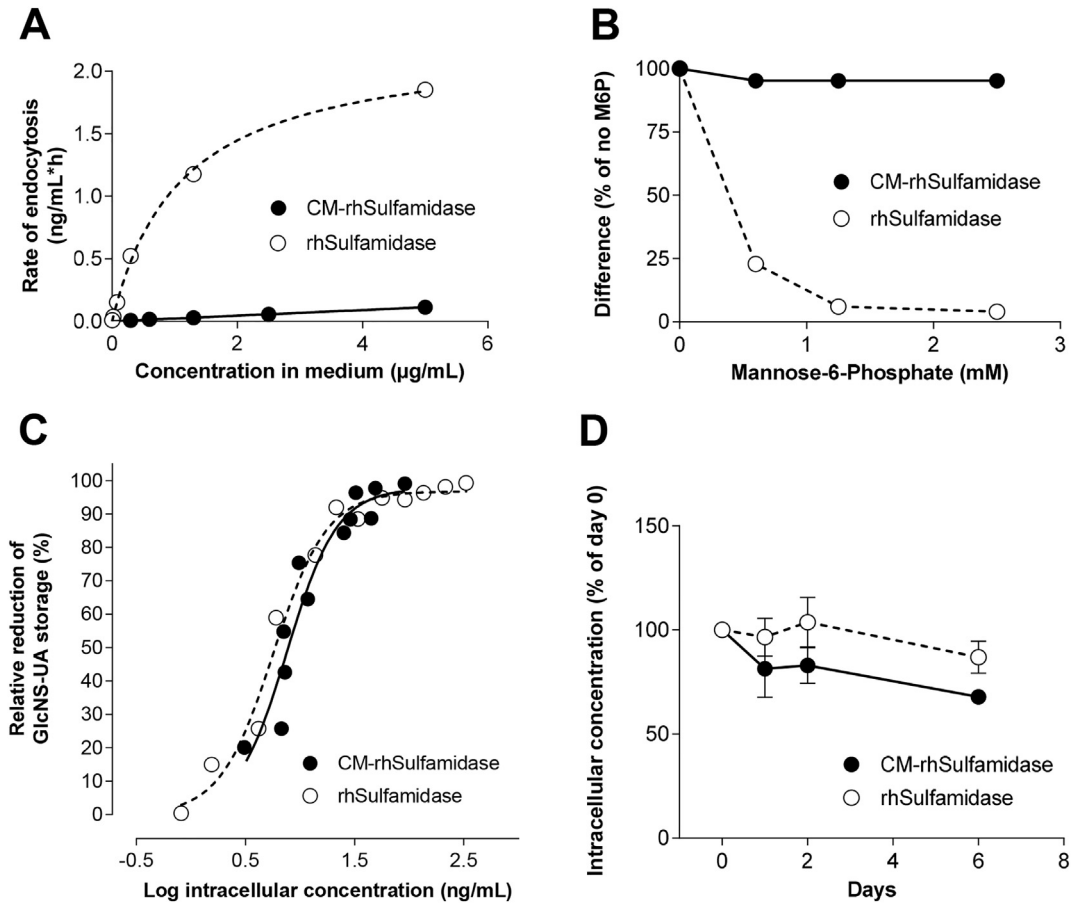


**Fig. 3.** *In vitro* characterization of CM-rhSulfamifdase and rhSulfamidase in primary MPS IIIA patient fibroblasts. (A) Endocytosis rate as a function of concentration. (B) M6P inhibition of endocytosis. (C) Concentration-dependent reduction of HS storage. (D) Intracellular retention and stability.

observed in cultured MPS IIIA patient fibroblasts was studied. Treatment effects of CM-rhSulfamidase or rhSulfamidase on HS levels were assessed by measuring the levels of the HS biomarker GlcNS-UA using LC-MS/MS. A 24-h incubation with CM-rhSulfamidase or rhSulfamidase reduced the HS biomarker GlcNS-UA in a concentration-dependent manner. CM-rhSulfamidase was equally efficient as rhSulfamidase in reducing the GlcNS-UA levels (Fig. 3C). A sigmoidal function with variable slope was fitted to the concentration response data. The intracellular $EC_{50}$ values of 8 ng/mL (0.15 nmol/L) or 6 ng/mL (0.11 nmol/L) and hillslope of 1.7 were not significantly different between CM-rhSulfamidase and rhSulfamidase.

To study intracellular retention, MPS IIIA patient fibroblasts were incubated with CM-rhSulfamidase at 2.5 µg/mL or rhSulfamidase at 0.05 µg/mL for 24 h to reach comparable intracellular levels at day 0. Extracellular CM-rhSulfamidase and rhSulfamidase were removed by a thorough washing procedure and intracellular concentrations were subsequently determined at different time points. CM-rhSulfamidase exhibited the same intracellular retention and stability as rhSulfamidase. The intracellular concentrations were only marginally reduced up to six days after treatment, CM-rhSulfamidase slightly more than rhSulfamidase (Fig. 3D). Thus, the intracellular stability and the HS degrading efficiency were not affected by the applied chemical modification.

### 3.4. Long systemic exposure of CM-rhSulfamidase after i.v. administration in mouse

The impact of chemical modification on the plasma concentration *versus* time profile was investigated in C57BL/6 mice following a single i.v. dose at 12 mg/kg (Fig. 4). At 5 min after administration the plasma

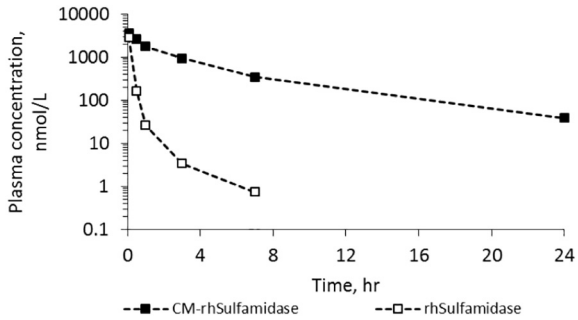


**Fig. 4.** Plasma concentration *versus* time following i.v. administration of 12 mg/kg rhSulfamidase or CM-rhSulfamidase in WT mice. Log-linear mean plasma concentration *versus* time profiles of rhSulfamidase and CM-rhSulfamidase in male C57BL/6 mice following a single 12 mg/kg i.v. dose ($n = 3$ samples per time point; Standard deviation error bars are included but are smaller than the symbol size).

concentration was slightly lower for rhSulfamidase relative to CM-rhSulfamidase, 2.7 *versus* 3.6 µmol/L (Table 1). Thereafter the rhSulfamidase plasma concentration declined rapidly in a distribution phase before entering a more stable terminal phase. Plasma clearance was > 10-fold higher for rhSulfamidase, 261 mL/h/kg, than for CM-rhSulfamidase, 19 mL/h/kg.

### 3.5. Effect of CM-rhSulfamidase on HS levels in MPS IIIA mice

The functional characteristics of CM-rhSulfamidase encouraged further evaluation of the compound, hence four pharmacological

**Table 1**
PK parameters of rhSulfamidase and CM-rhSulfamidase dosed 12 mg/kg i.v. in C57BL/6 mice.

| Compound | $t_{max}$ (h) | $C_{max}$ (μmol/L) | $C_{last}$ (nmol/L) | $AUC_{last}$ (h*μmol/L) | $V_z$ (mL/kg) | CL (mL/h/kg) | $V_{ss}$ (mL/kg) |
|---|---|---|---|---|---|---|---|
| CM-rhSulfamidase | 0.08 | 3.6 | 38.5 | 10.2 | 127 | 19 | 99 |
| rhSulfamidase | 0.08 | 2.7 | 0.7 | 0.74 | 466 | 261 | 66 |

Abbreviations: $t_{max}$, time at which $C_{max}$ was reached; $C_{max}$, maximum concentration; $C_{last}$, last observed concentration above LLOQ; $AUC_{last}$, area under the concentration-time curve from $t = 0$ to the last observed concentration; $V_Z$, volume of distribution of the terminal phase; CL, clearance; $V_{SS}$, volume of distribution at steady state.

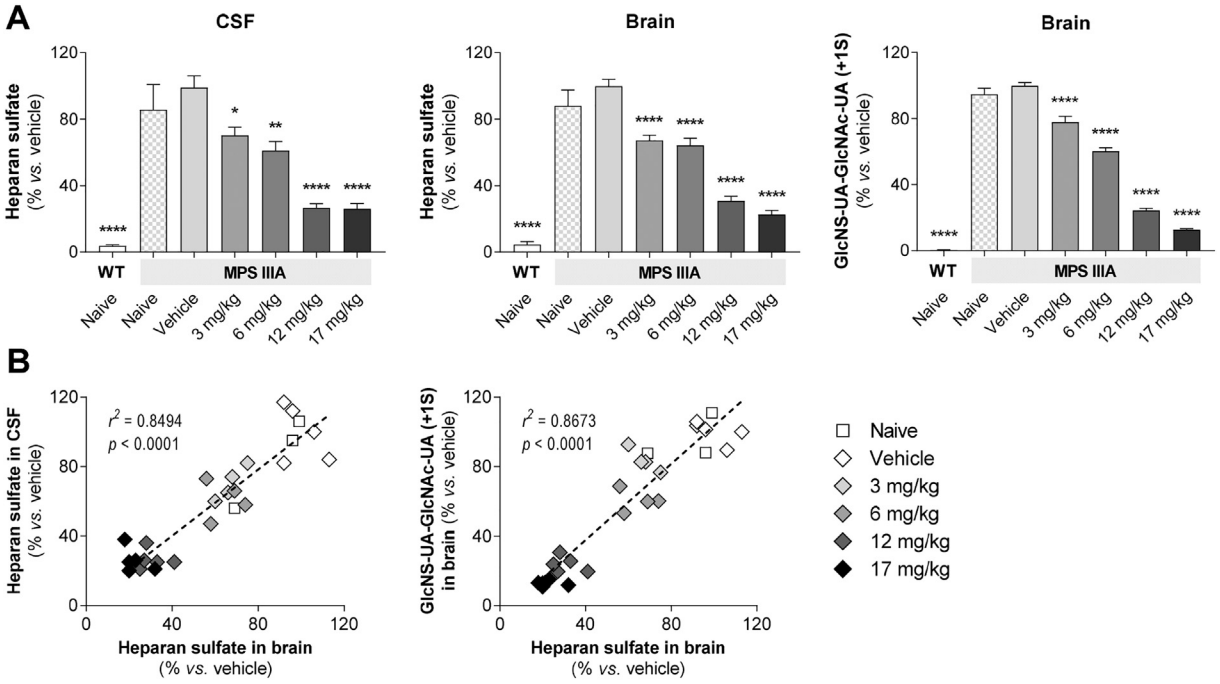


**Fig. 5.** Effect of CM-rhSulfamidase on HS levels in CNS of MPS IIIA mice. Relative levels of HS and a HS-derived tetrasaccharide, GlcNS-UA-GlcNAc-UA (+1S), in CSF and brain homogenate samples from MPS IIIA mice at 29 weeks of age after i.v. administration of vehicle or CM-rhSulfamidase at 3, 6, 12 or 17 mg/kg once weekly for 20 weeks ($n$ = 2–8). Naïve MPS IIIA and WT mice were included as controls. (A) Results are shown as group mean (± SEM). One-way ANOVA and *post hoc* Dunnett's test *versus* vehicle; *$p < .05$, **$p < .01$, ***$p < .001$, and ****$p < .0001$. (B) Individual data are presented. Pearson's correlation is illustrated with $r^2$ and $p$ values in the figure.

studies in male MPS IIIA mice (Study A-D) were performed. Due to low residual sulfamidase activity, MPS IIIA mice exhibit extensive accumulation of HS and an HS-derived tetrasaccharide, GlcNS-UA-GlcNAc-UA (+1S), in the CNS compared to WT mice (Fig. 5A). Intravenous administration of CM-rhSulfamidase to MPS IIIA mice at 3, 6, 12 or 17 mg/kg once weekly for 20 weeks (Study B) resulted in statistically significant dose-dependent reductions of these stored substrates (Fig. 5A). The HS level in CSF correlated with the HS level in brain in individual mice, and the reduction of HS correlated with the reduction of GlcNS-UA-GlcNAc-UA (+1S) in brain (Fig. 5B). A shorter treatment duration was also evaluated (Study A). Brain levels of the HS-derived tetrasaccharide GlcNS-UA-GlcNAc-UA (+1S) were reduced by 30 and 70% *versus* vehicle controls in MPS IIIA mice that received 10 weekly injections of CM-rhSulfamidase at 6 or 18 mg/kg (data not shown). A complete normalization of GlcNS-UA-GlcNAc-UA (+1S) levels occurred in liver at all dose levels tested (data not shown).

Additional studies with repeated i.v. administration of CM-rhSulfamidase to MPS IIIA mice, showed that 20 weekly injections of CM-rhSulfamidase at a higher dose (22 mg/kg, Study C) reduced the CNS levels of HS further, reaching 80 to 90% reduction *versus* vehicle controls. Eight weeks after the final dose of CM-rhSulfamidase, the levels of HS in CNS were still reduced by 40 to 50%, followed by approximately 20% reduction at 16 weeks after the final dose, demonstrating slowly increasing HS levels when treatment was discontinued (Fig. 6). Brain levels of GlcNS-UA-GlcNAc-UA (+1S) followed the same pattern as HS and were also reduced to similar levels by CM-rhSulfamidase treatment (data not shown).

Development of ADA responses against CM-rhSulfamidase was monitored in MPS IIIA mice after repeated i.v. administration of CM-rhSulfamidase at 7 mg/kg for 25 weeks (Study D). Cohorts of vehicle- and CM-rhSulfamidase-treated mice were pre-treated with the immune system suppressant MTX to reduce ADA responses. Transient ADA responses were apparent in animals that received CM-rhSulfamidase without MTX pre-treatment, whereas pre-treatment attenuated or prevented ADA development. Levels of GlcNS-UA-GlcNAc-UA (+1S) in brain were reduced by 60 and 70% *versus* vehicle controls, with or without MTX pre-treatment (data not shown). Thus, the efficacy of CM-rhSulfamidase was not significantly affected by the MTX pre-treatment, suggesting that the ADA response was non-neutralizing.

### 3.6. Effect of CM-rhSulfamidase on brain pathology in MPS IIIA mice

Ceroid- and lipofuscin cytoplasmic and lysosomal inclusions within the brain emit autofluorescent (AF) signals in a broad wavelength spectrum that can be detected by epifluorescence microscopy [51,52]. The AF load in brain is increased in MPS pathology and MPS IIIA mice, being located mainly in neurons [30,47]. In 19-week-old MPS IIIA mice, a 4-fold increase of the AF signal was found in cortex and hippocampus

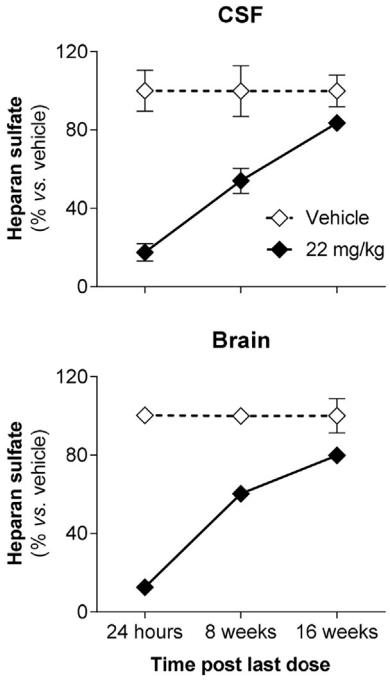


**Fig. 6.** HS levels in brain of MPS IIIA mice 24 h, 8 and 16 weeks after discontinuation of treatment with CM-rhSulfamidase. Relative levels of HS in CSF and brain homogenate samples from male MPS IIIA mice at 30 to 46 weeks of age after i.v. administration of vehicle or CM-rhSulfamidase at 22 mg/kg once weekly for 20 weeks ($n$ = 3–8). Results are shown as group mean ( ± SEM).

*versus* WT mice (Fig. 7A-B). In cerebellum, high basal AF levels in WT mice were not significantly lower than MPS IIIA vehicle controls (Fig. 7C). Intravenous administration of CM-rhSulfamidase to male MPS IIIA mice at 6 or 18 mg/kg once weekly for 10 weeks (Study A) resulted in a significant dose-dependent reduction of the AF signal in cortex and hippocampus *versus* vehicle control (Fig. 7A-B), while only the highest dose level gave a reduction in cerebellum (Fig. 7C).

To further evaluate the effect of repeated CM-rhSulfamidase administration on lysosomal storage and pathology, the size of the lysosomal compartment was analyzed by immunohistochemical detection of the integral lysosomal membrane protein, LIMPII, in the same cohort of mice (Study A). CM-rhSulfamidase at 18 mg/kg for 10 weeks reduced the density of the LIMPII positive signals in cortex and hippocampus *versus* vehicle control, whereas no effect on lysosomal compartment size was found in cerebellum (Fig. 8).

Effect of treatment on neuroinflammation was evaluated in MPS IIIA mice after 10 or 25 weeks repeated administration of CM-rhSulfamidase (Study A and Study D). Astrogliosis was assessed using the astrocyte marker glial fibrillary acidic protein (GFAP). The results recapitulated the reported disease phenotype [47] with increased density of reactive astrocytes in cerebral cortex and hippocampus in MPS IIIA mice compared to WT mice (Fig. 9A-B). Repeated administration of CM-rhSulfamidase at 7 mg/kg for 25 weeks to MSP IIIA mice (Study D) resulted in a significant reduction of GFAP-positive immunoreactivity, close to WT levels in cortex and hippocampus, *versus* vehicle control (Fig. 9B).

Microgliosis was assessed by two different markers, allograft inflammatory factor 1 (Iba-1) and CD11b, with similar results. Reported herein, an almost 2-fold increase in mean size of CD11b-positive microglial objects was observed in MPS IIIA mice compared to WT mice (Fig. 9C). The microglia object size was significantly reduced in cerebral cortex in MPS IIIA mice by weekly CM-rhSulfamidase treatment at

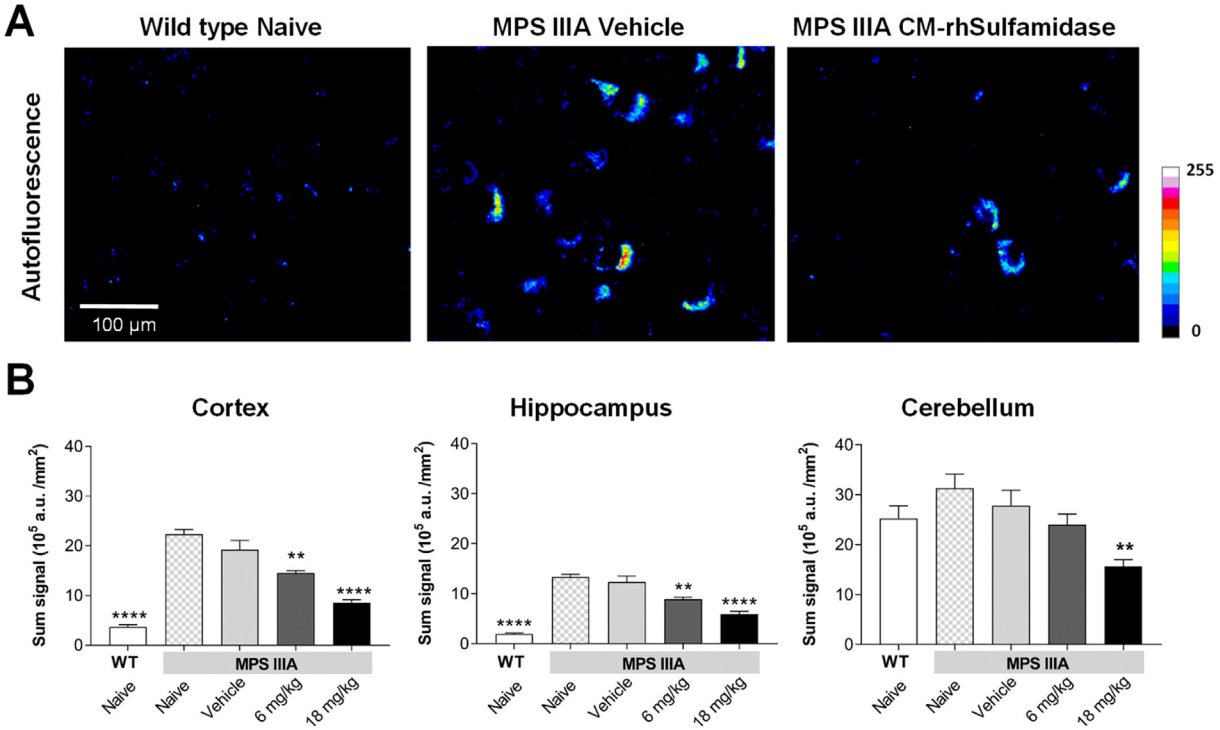


**Fig. 7.** Autofluorescing intracellular inclusions in brain of male MPS IIIA mice at 19 weeks of age after i.v. administration of vehicle or CM-rhSulfamidase at 6 or 18 mg/kg once weekly for 10 weeks ($n$ = 5–6). Naïve MPS IIIA and WT mice were included as controls. (A) Representative photomicrographs from the cerebral cortex layer IV/V acquired at 10× (numerical aperture N.A. 0.45) using long exposure (600 ms) epifluorescence microscopy. Scale bar 100 µm. Signal intensities shown in a pseudocolor scale (0–255). (B) AF inclusions quantified as sum of signal intensity arbitrary unit (a.u.) per area unit in cortex, hippocampus and cerebellum. Results are shown as group mean ( ± SEM) sum of signal per mm$^2$. One-way ANOVA and *post hoc* Dunnett's test *versus* vehicle; *$p$ < .05, **$p$ < .01, ***$p$ < .001, and ****$p$ < .0001. .

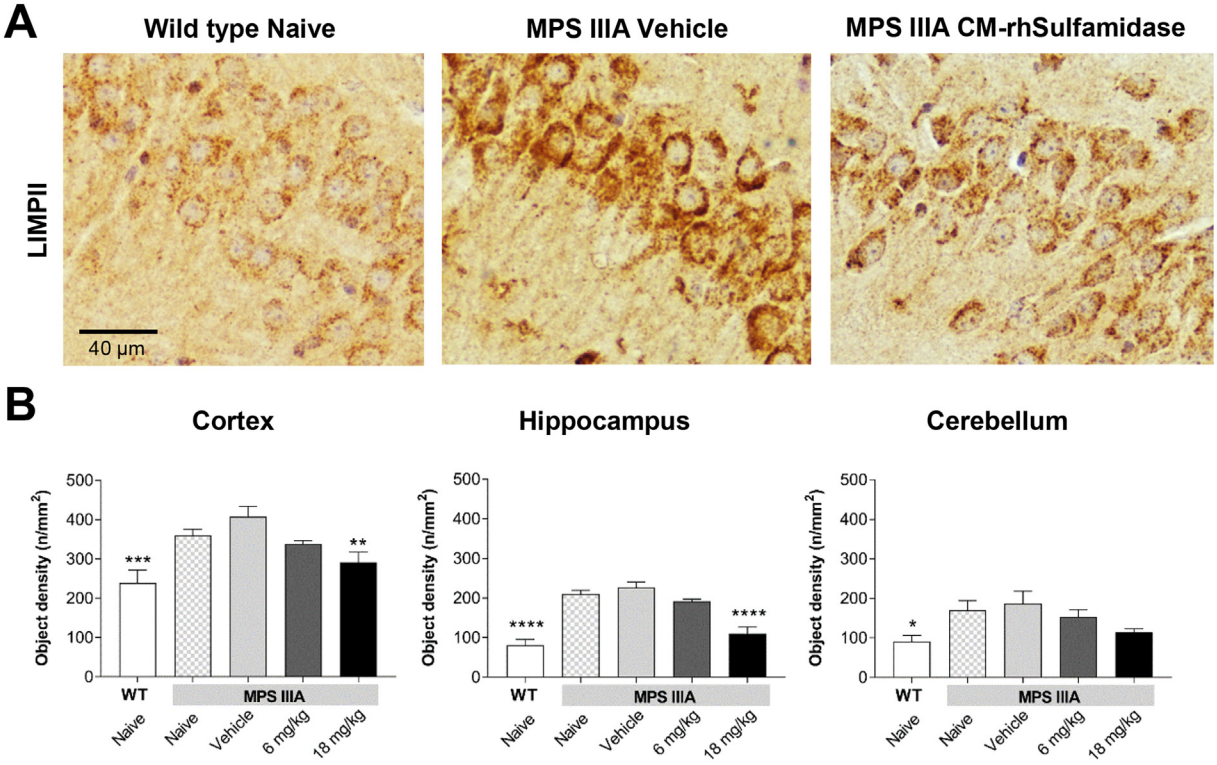


**Fig. 8.** Immunohistochemical detection of the lysosomal integral membrane protein (LIMPII) in MPS IIIA mouse brain after repeated i.v. administration of vehicle or CM-rhSulfamidase. Naïve MPS IIIA and WT mice were included as controls. (A) Representative photomicrographs from the hippocampal cell layer in male mice treated with CM-rhSulfamidase at 22 mg/kg for 20 weeks ($n = 8$). Paraffin sections counterstained with hematoxylin acquired at 20× (numerical aperture N.A. 0.40). Scale bar 40 µm. (B) LIMPII-positivity quantifications from cortex, hippocampus and cerebellum in male mice treated with CM-rhSulfamidase at 6 or 18 mg/kg for 10 weeks ($n = 5$–6), using image segmentation analysis. Results are shown as group mean ( ± SEM) of object density per $mm^2$. One-way ANOVA and *post hoc* Dunnett's test *versus* vehicle; $^*p < .05$, $^{**}p < .01$, $^{***}p < .001$, and $^{****}p < .0001$.

7 mg/kg for 25 weeks (Study D), and almost normalized to WT levels in hippocampus when compared to vehicle controls (Fig. 9C). Reduction of astrogliosis and microgliosis was also observed after administration of CM-rhSulfamidase at 18 mg/kg for 10 weeks (Study A).

### 3.7. Effect of CM-rhSulfamidase on behavioral impairments in MPS IIIA mice

Exploratory behavior of male MPS IIIA mice in a novel environment was tested during 5 min in an open field arena. The test was performed at 27 to 28 weeks of age after i.v. administration of CM-rhSulfamidase at 3, 6, 12 or 17 mg/kg (Study B) or 22 mg/kg (Study C) once weekly for 20 weeks. Male MPS IIIA mice displayed reduced activity compared to WT controls, and a significant improvement of the time spent active (speed > 5 m/s) was shown at the highest dose of CM-rhSulfamidase (Fig. 10A). Trends towards increased activity did not reach statistical significance after correction for group comparisons for the other parameters evaluated (Fig. 10A), or at lower doses (data not shown).

Neuromuscular function of male MPS IIIA mice was assessed by a wire hanging test. Aged MPS IIIA mice (34 weeks of age, Study D) demonstrated a clear phenotype with reduced hanging performance. This impairment of performance was almost completely corrected to normal levels after i.v. administration of CM-rhSulfamidase at 7 mg/kg once weekly for 25 weeks (Fig. 10B). At a slightly younger age (29 weeks of age, Study B), vehicle treated MPS IIIA mice tended to drop at the same time as naïve MPS IIIA mice. Treatment of MPS IIIA mice with CM-rhSulfamidase at 3, 6, 12 or 17 mg/kg once weekly for 20 week resulted in an increase of wire hanging time to similar levels as WT mice, but the treatment effect did not reach statistical significance after correction for group comparisons (data not shown).

Social ability of male MPS IIIA mice was tested at 29 to 30 weeks of age in a three-chamber social interaction test, after i.v. administration of CM-rhSulfamidase at 22 mg/kg once weekly for 20 weeks (Study C). During the social approach session, a novel mouse intruder was placed in one of three chambers, whereas both a familiar and a novel intruder were placed in separate chambers during the social novelty session. Mice normally prefer to spend more time with another mouse (sociability), and will investigate a novel intruder more than a familiar one (social novelty). During the social approach session, MPS IIIA mice demonstrated a reduced sociability that was normalized by treatment with CM-rhSulfamidase (Fig. 10C). During the social novelty session MPS IIIA mice failed to demonstrate a clear phenotype *versus* WT mice resulting in the inability to evaluate treatment effect.

Learning ability of the same animals as used above (Study C), was assessed in a Barnes maze test at 28 to 29 weeks of age. This test is a dry-land maze test for spatial learning and memory where animals escape from a brightly lit, exposed circular open platform surface to a small, dark recessed target chamber located under one of 20 holes around the perimeter of the platform. Four learning trials on each of four consecutive days were performed. MPS IIIA mice treated with CM-rhSulfamidase behaved similarly to WT mice, and performed better compared to MPS IIIA mice receiving vehicle (Fig. 10D). Twenty-four hours after the last learning trial on day four, mice were tested for short-term memory in the probe trial. MPS IIIA mice presented weak memory deficits that improved after CM-rhSulfamidase treatment, although the difference failed to reach statistical significance when compared to vehicle treated controls (Fig. 10D).

### 3.8. Presence and localization of CM-rhSulfamidase in CNS

Distribution of CM-rhSulfamidase to brain was confirmed by concentration determinations in homogenate of saline perfused MPS IIIA

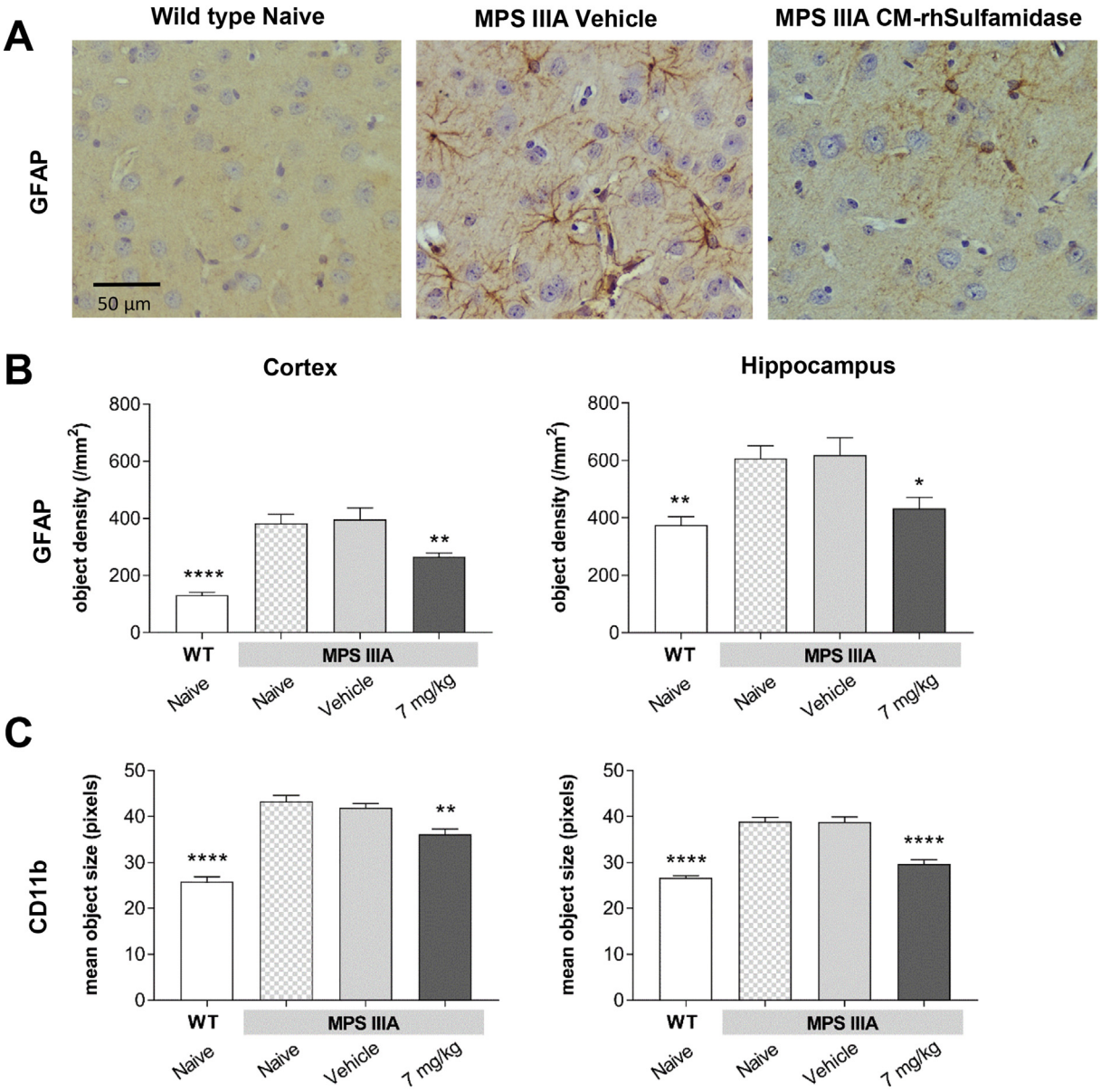


**Fig. 9.** Neuroinflammation in the MPS IIIA mouse brain after repeated i.v. administration of vehicle or CM-rhSulfamidase. Naïve MPS IIIA and WT mice were included as controls. (A) Representative bright field photomicrographs from the cortex in male mice treated with CM-rhSulfamidase at 22 mg/kg for 20 weeks ($n = 8$). Paraffin sections counterstained with hematoxylin acquired at 20× (numerical aperture N.A. 0.40). Scale bar 50 µm. (B–C) Quantification of GFAP positive astrocytes and CD11b positive microglia in cortex and hippocampus in male mice treated with CM-rhSulfamidase at 7 mg/kg for 25 weeks ($n = 8$). Results are shown as group mean values ( ± SEM) of object density per $mm^2$ (GFAP) or mean object size of each positive object (CD11b). One-way ANOVA and *post hoc* Dunnett's test *versus* vehicle; *$p < .05$, **$p < .01$, ***$p < .001$, and ****$p < .0001$.

mouse brains obtained at 24 h after the last dose (Study B; Fig. 11). Concentrations of CM-rhSulfamidase in brain were 100-fold lower than in serum.

Presence of CM-rhSulfamidase in brain was further investigated by immunohistofluorescent detection in a cohort of MPS IIIA mice treated for 10 weeks with CM-rhSulfamidase at 6 or 18 mg/kg, using vehicle-treated MPS IIIA mice and untreated WT mice as controls (Study A). The antibody used was raised against CM-rhSulfamidase, but also recognizes endogenous WT mouse sulfamidase (supplementary Fig. 1). Qualitative inspection revealed strong signals from meninges, in the walls of arterioles and larger blood vessels of the brain, but also very distinctly around the profiles of smaller vessels, in mice treated with 18 mg/kg (Fig. 12A). These signals were less frequent and of lower intensity in mice treated at 6 mg/kg, and absent in vehicle-treated and naïve MPS IIIA animals. In WT mice, signals were equally strong but fewer and in a more punctate pattern. Signals were quantified in predefined areas of interest (cortex, hippocampus and cerebellum) and categorized into compartments defined as vascular, parenchymal and that overlapping autofluorescent (AF) objects (see *Supplementary Methods* and *Results*). The quantitative analysis revealed presence of CM-rhSulfamidase in vascular like structures in cortex (Fig. 12B), hippocampus and cerebellum (supplementary Fig. 2) in MPS IIIA mice treated with 18 mg/kg CM-rhSulfamidase (24 h after the last dose). In WT mice, signals were significantly elevated above vehicle-treated MPS IIIA mice in both cortex (Fig. 12B) and hippocampus (supplementary Fig. 2). In the parenchymal compartment, signals were less strong, the total signal being 13-fold higher in mice treated with CM-rhSulfamidase at 18 mg/kg compared to vehicle-treated controls (Fig. 12B). The lower dose of 6 mg/kg failed to show significant signal above control levels. In the area which overlapped with AF, specific signal from sulfamidase

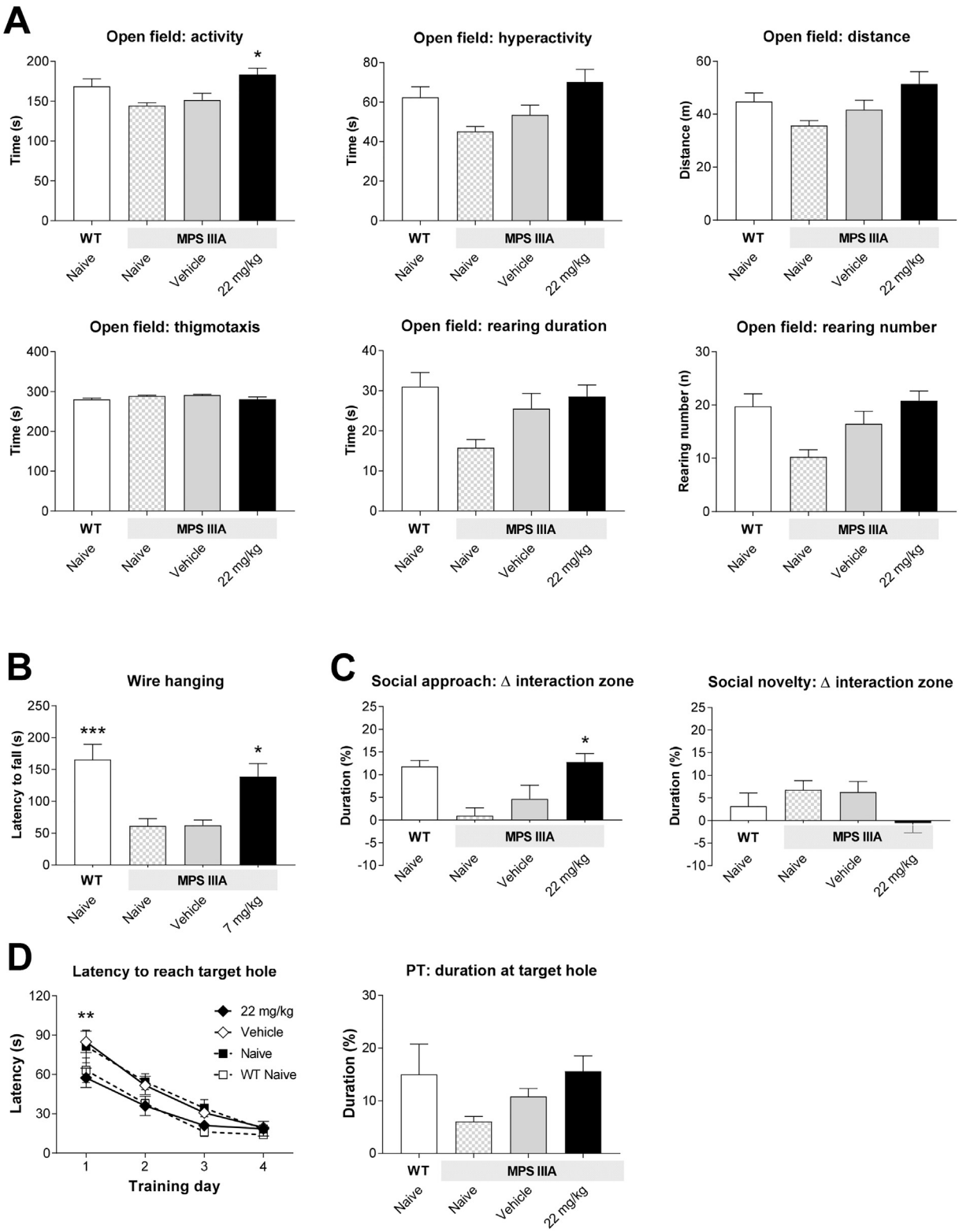


**Fig. 10.** Effect of CM-rhSulfamidase on behavioral impairments in MPS IIIA mice. (A) Exploratory activity assessed by the open field test using male mice from Study C at 27 to 28 weeks of age. Graphs illustrate active time (speed > 5 m/s), hyperactive time (speed > 15 m/s), total distance travelled, time spent in the periphery (thigmotaxis), rearing number, and time spent rearing. A total experiment duration of 5 min was used. (B) Neuromuscular function assessed by the wire hanging test using male mice from Study D at 34 weeks of age. Graph illustrates total time the animals were able to hold themselves on the wire grid. The result was the same if body weight was taken into account. (C) Social ability assessed by the three-chamber social interaction test using male mice from Study C at 29 to 30 weeks of age. Graphs illustrate the delta of the interaction duration during the social approach (stranger *versus* empty) and social novelty (stranger *versus* familiar) sessions of the test. An experiment duration of 10 min was used for the different sessions. (D) Learning ability assessed by the Barnes maze test using male mice from Study C at 28 to 29 weeks of age. Graphs illustrate the latency to find the target hole per day during the learning trials of the test and relative duration at the target hole during the probe trial (PT). Results are shown as group mean ( ± SEM) of $n = 8–16$. One- or two-way ANOVA and *post hoc* Dunnett's test *versus* vehicle; $*p < .05$, $**p < .01$, and $***p < .001$.

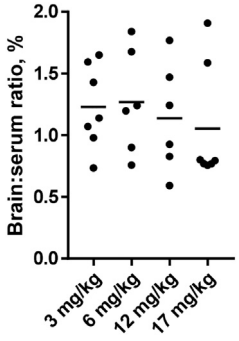


**Fig. 11.** CM-rhSulfamidase concentration ratio in brain homogenate *versus* serum at 24 h after the last of 20 i.v. doses given once weekly to MPS IIIA mice (Study B). Individual data with mean are presented.

was of higher mean intensity (data not shown) and of 2- to 3-fold higher density in MPS IIIA mice treated with CM-rhSulfamidase compared to vehicle-treated MPS IIIA mice (Fig. 12C). Signal intensity analysis of the expanded rim (3 pixels increased perimeter) revealed stronger sulfamidase signals in WT mice and MPS IIIA mice receiving a high dose of CM-rhSulfamidase, while low signals were detected in naïve or vehicle-treated MPS IIIA mice (Fig. 12C).

## 4. Discussion

This study demonstrates improvement of CNS pathology in a MPS IIIA mouse model with a therapeutic approach using CM-rhSulfamidase that may be translational and clinically applicable. The basis for efficacy is a mild disruption of the glycan structure of sulfamidase, leaving enzymatic activity intact but reducing glycan mediated uptake into cells. The reduced cellular uptake resulted in a prolonged high exposure in plasma after i.v. administration of CM-rhSulfamidase, facilitating passage across the mouse BBB. Chronic systemic delivery of a high dose of CM-rhSulfamidase to MPS IIIA mice yielded up to 90% reduction of HS levels within the CNS compared to controls. This is in agreement with a study where high sustained circulating sulfamidase levels achieved by gene therapy targeting the liver, also significantly reduced CNS accumulation of HS [35]. The path of brain entrance is yet unclear, but a possible mechanism is passive transcytosis over the BBB. Pioneering studies by Grubb et al. showed that a glycan disruption procedure, similar to the one described here, increased serum exposure of β-glucuronidase, and resulted in efficient clearance of neuronal storage in an MPS VII mouse model [14]. In contrast, the same procedure applied to tripeptidyl peptidase in a mouse model of CLN3, and surprisingly to sulfamidase in a mouse model of MPS IIIA, did not improve therapeutic efficacy, indicating that the general applicability of this procedure is uncertain [28,34]. Transcytosis efficiency over the BBB may be dependent on the structure of the disrupted glycans. Both glycan pattern of the starting material and the conditions during the chemical modification procedure impact the final glycan composition, as illustrated by the N131 mannose 6-glycan of CM-rhSulfamidase in this study. The optimization of the chemical modification undertaken showed that harcher conditions, closer to those used by others previously, resulted in more substantial changes in the glycan structure but also in the polypeptide structure. Thus, the intrinsic biochemical properties has to be closely considered when to assess the applicability of the chemical modification approach for other lysosomal enzymes. The recombinant Sulfamidase produced in this study was remarkably stable, and both rhSulfamidase and CM-rhSulfamidase appeared to be retained within the cells, which agrees with studies of sulfamidase being poorly secreted from transduced cells [8,25]. The strong intracellular retention and stability may be key features enabling effective intra-lysosomal concentrations of CM-rhSulfamidase in CNS after repeated administration.

Our data on CNS pathology in the MPS IIIA mouse are in strong contrast to those obtained by Rozkalis et al. [53], reporting no effect of repeated dose treatment with rhSulfamidase or CM-rhSulfamidase. In addition to the differences in chemical modification protocol, leading to different products, a shorter study duration in combination with choise of biomarker could potentially have impact on outcome. In Rozkalis et al. [2011] GlcNS-UA was measured, while in this study effect of CM-rhSulfamidase on HS and the tetrasaccharide, GlcNS-UA-GlcNAc-UA (+1S), are presented. HS levels are determined after *in vitro* digestion of the total metabolite pool before comparison to 4 different disaccharide standards, and thus includes the native disaccharide pool as well as higher saccharide species. CM-rhSulfamidase treatment might initially result in a reduction of especially the higher saccharide species thereby producing lower saccharide species. In support of this is the observation that in liver the effect of CM-rhSulfamidase treatment was lower on GlcNS-UA levels as compared with GlcNS-UA-GlcNAc-UA (+1S) levels and a low single dose of CM-rhSulfamidase even resulted in an increase of GlcNS-UA [26]. Thus, enzyme stability and activity, study duration, dose level and frequency and the biomarker might all have contributed to the clear effect on biomarkers in brain in our studies.

To support the quantitative concentration data obtained from homogenized brain tissue confirming distribution of systemically administered CM-rhSulfamidase to brain, presence of CM-rhSulfamidase was further studied by immunhistofluorescent detection in anatomically defined structures sampled throughout the brain after repeated i.v. dosing of CM-rhSulfamidase. The antibody used detected both endogenous sulfamidase and CM-rhSulfamidase, but in MPS IIIA mice these endogenous levels are low (undetectable). Cytoplasmic compartments of neurons including lysosomes can be identified by autofluorescence from the cerebral cortex of MPS III mice and patients [27],31,36]. Indirect evidence that CM-rhSulfamidase reached the target compartment in brain, was its co-localization with the autofluorescing cytoplasmic inclusions. Antibody signals located within and in close vicinity to dense autofluorescent perinuclear particles were clearly above the baseline signal in naïve or vehicle-treated MPS IIIA mice. These findings, together with the evident efficacy on lysosomal compartment size, point towards an efficient target engagement in the lysosomes of brain cells.

MPS IIIA mice are known to closely recapitulate the human disease, presenting accumulation of HS from birth, behavioral abnormalities, neuroinflammation, neurodegeneration, and a shortened lifespan [9,16,35,47]. The dose-dependent reduction of HS levels in brain after once weekly i.v. administration of CM-rhSulfamidase as reported in this paper was accompanied by a decrease in neuroinflammation. Activation of microglia documented in several MPS pathologies [30,47,54] has a negative impact on neurodegeneration [2]. Although the mechanisms behind neuroinflammation in MPS pathologies are not fully understood, emerging evidence suggests that a decrease in inflammation can be disease-modifying by itself, contributing to both reduced pathology and behavioral deficits [32].

Neurodegeneration in MPS IIIA mice is reflected in progressive motor and learning deficits [13,17,9]. In this study, behavioral impairments were evaluated in different behavioral tests. The evaluation was exploratory since the experiments were not powered for full behavioral readouts. Nevertheless, the results indicate that reduction of HS in brain was associated with improvements in behavioral phenotype. Systemic delivery of CM-rhSulfamidase to MPS IIIA mice restored normal wire hanging capabilities. This improvement in motor function agrees with previous reports of improved righting response [20] and rotarod performance [6] in sulfamidase-treated MPS IIIA mice. Male MPS IIIA mice monitored in an open field test demonstrated a hypoactive phenotype consistent with previous findings [16,24,40]. The hypoactivity was improved by CM-rhSulfamidase, which is in agreement with other reports showing increased exploratory activity after sulfamidase ERT [17] or gene transfer [40]. Sociability status and social

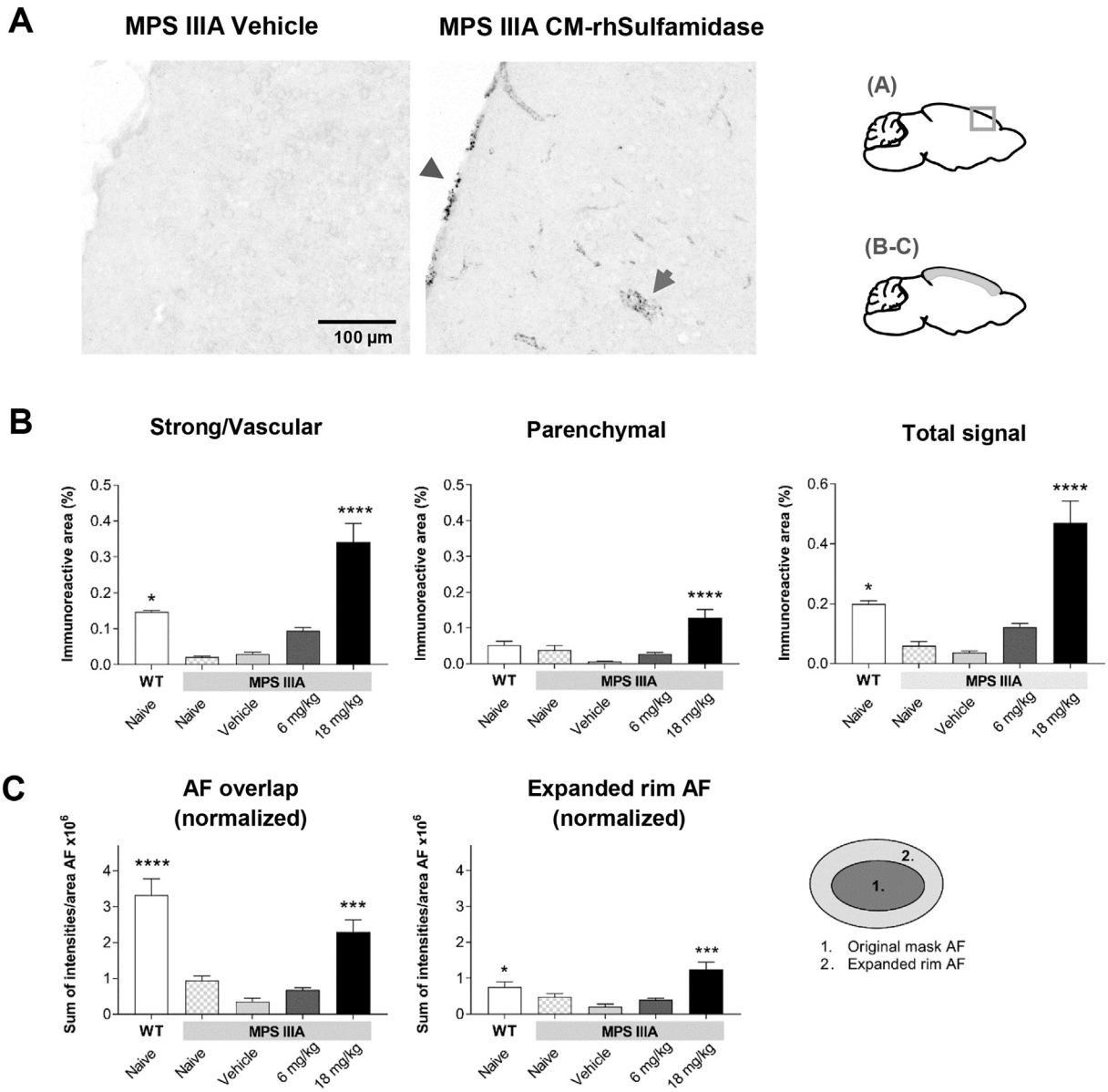


**Fig. 12.** Immunohistological localization of Sulfamidase in the cerebral cortex of male MPS IIIA mice treated with vehicle or CM-rhSulfamidase at 6 or 18 mg/kg once weekly for 10 weeks ($n$ = 4–6). Naïve MPS IIIA mice and WT mice were included as controls. (A) Representative inverted greyscale photomicrographs of CM-rhSulfamidase fluorescent (−647) signal from the superficial cortical layers of a vehicle- or CM-rhSulfamidase-treated mouse (18 mg/kg). The arrowhead points to the strong meningeal signal and the arrow to an immunopositive arteriole. Scale bar 100 µm. (B) Quantification of strong signals classified to a "vascular" mask (left graph), weaker signal intensities classified as "parenchymal" (mid graph) and sum of vascular and parenchymal signals (right graph). (C) Quantification of signal above threshold localized to AF inclusions (left) and to an expanded rim from the AF masked objects (3 pixels ≈ 1.94 µm) as depicted schematically to the bottom right. All values normalized to the total AF object area (*i.e.* mean sum of signal per autofluorescing area unit). Results are shown as group mean ( ± SEM). One-way ANOVA and *post hoc* Dunnett's test *versus* vehicle; $*p < .05$, $***p < .001$, and $****p < .0001$. One outlier was excluded from the vehicle group from all datasets based on Grubb's outlier analysis.

novel preference of MPS IIIA mice were investigated using a three-chamber social interaction test as previously described for MPS II mice [Gleitz 2017]. MPS IIIA mice demonstrated a reduced sociability that was normalized by treatment with CM-rhSulfamidase. The social novel preference revealed no significant differences between MPS IIIA and WT mice. Finally, consistent with previous findings using the Morris water maze [13,16,12], MPS IIIA mice treated with CM-rhSulfamidase behaved similar to WT mice and performed better compared to MPS IIIA control mice during the learning trials in a Barnes maze test. They also presented weak memory deficits that improved after treatment, although the improvement did not reach statistical significance compared to controls. A larger sample size would be needed to confirm the effect of CM-rhSulfamidase on some behavioral readouts.

To our knowledge, this is the first study to measure HS in CSF of MPS IIIA mice. The levels of HS were high but decreased after CM-rhSulfamidase treatment in a manner directly proportional to the reduction seen in brain homogenates. A similar correlation between HS levels in brain and CSF is seen with ERT in the mouse model of MPS II utilizing a transferrin receptor targeting iduronidase fusion [Tanaka 2018]. HS in CSF is particularly interesting as a disease marker since it is assessable in clinical studies and can confirm pharmacological activity in the CNS compartment. To what extent different cells and anatomical regions of the brain contribute to the HS present in CSF is still largely unclear. However, the possibility that HS from peripheral tissues contributes *via* blood-CSF transfer can be ruled out in the MPS IIIA mouse model since the HS level in blood was normalized more

rapidly and at significantly lower doses of CM-rhSulfamidase (data not shown). Although clinical data suggest that the predictive value of HS in CSF may be limited for ERT administrated directly into CSF [19,46], or gene therapy locally administrated in the brain parenchyma [41], preclinical data in this study suggest that HS in CSF is a relevant marker for i.v. administrated CM-rhSulfamidase in the clinical setting.

## 5. Conclusion

In summary, the pharmacological *in vivo* data demonstrated that systemically administered CM-rhSulfamidase reduced HS storage in brains of MPS IIIA mice. This reduction of HS storage was associated with reduced neuroinflammation and a trend towards improved behavioral outcomes in MPS IIIA mice. The analogy of the disease progression in MPS IIIA mice to that in patients provide support for the translation of this approach to treatment of patients with MPS IIIA. Clinical studies evaluating safety and efficacy of a CM-rhSulfamidase are currently ongoing (NCT03423186 & NCT03811028).

## Funding

This study was fully funded by Swedish Orphan Biovitrum AB (publ).

## Disclosures

All authors are employees (or former employees) of Swedish Orphan Biovitrum AB (publ) which is developing CM-rhSulfamidase as a potential commercial therapeutic agent. All authors declare equity interest in Swedish Orphan Biovitrum AB (publ).

## Acknowledgements

The authors wish to thank the Sobi team responsible for developing the process and producing the CM-rhSulfamidase for the studies. Further, the authors thank Drs. Charlotte Söderberg Nyhem and Stephen James for their contribution to the conception of Study A, supervision, and manuscript review. The excellent support of the contract research organization QPS Neuropharmacology in Austria is also acknowledged.

## Appendix A. Supplementary data

Supplementary data to this article can be found online at https://doi.org/10.1016/j.ymgmr.2019.100510.

## References

[1] L.D. Archer, K.J. Langford-Smith, B.W. Bigger, J.E. Fildes, Mucopolysaccharide diseases: a complex interplay between neuroinflammation, microglial activation and adaptive immunity, J. Inherit. Metab. Dis. 37 (2014) 1–12.
[2] J. Ausseil, N. Desmaris, S. Bigou, R. Attali, S. Corbineau, S. Vitry, M. Parent, D. Cheillan, M. Fuller, I. Maire, M.T. Vanier, J.M. Heard, Early neurodegeneration progresses independently of microglial activation by heparan sulfate in the brain of mucopolysaccharidosis IIIB mice, PLoS One 3 (2008) e2296.
[3] H. Beard, S. Hassiotis, W.P. Gai, E. Parkinson-Lawrence, J.J. Hopwood, K.M. Hemsley, Axonal dystrophy in the brain of mice with Sanfilippo syndrome, Exp. Neurol. 295 (2017) 243–255.
[4] R. Bhattacharyya, B. Gliddon, T. Beccari, J.J. Hopwood, P. Stanley, A novel missense mutation in lysosomal sulfamidase is the basis of MPS III A in a spontaneous mouse mutant, Glycobiology 11 (2001) 99–103.
[5] M. Bhaumik, V.J. Muller, T. Rozaklis, L. Johnson, K. Dobrenis, R. Bhattacharyya, S. Wurzelmann, P. Finamore, J.J. Hopwood, S.U. Walkley, P. Stanley, A mouse model for mucopolysaccharidosis type III A (Sanfilippo syndrome), Glycobiology 9 (1999) 1389–1396.
[6] R.J. Boado, J.Z. Lu, E.K. Hui, W.M. Pardridge, Reduction in brain heparan sulfate with systemic administration of an IgG Trojan horse-sulfamidase fusion protein in the mucopolysaccharidosis type IIIA mouse, Mol. Pharm. 15 (2018) 602–608.
[7] D. Buhrman, K. Thakkar, M. Poe, M.L. Escolar, Natural history of sanfilippo syndrome type A, J. Inherit. Metab. Dis. 37 (2014) 431–437.
[8] Y. Chen, S. Zheng, L. Tecedor, B.L. Davidson, Overcoming limitations inherent in sulfamidase to improve mucopolysaccharidosis IIIA gene therapy, Mol. Ther. 26 (2018) 1118–1126.
[9] A.C. Crawley, B.L. Gliddon, D. Auclair, S.L. Brodie, C. Hirte, B.M. King, M. Fuller, K.M. Hemsley, J.J. Hopwood, Characterization of a C57BL/6 congenic mouse strain of mucopolysaccharidosis type IIIA, Brain Res. 1104 (2006) 1–17.
[10] U. Dunder, V. Kaartinen, P. Valtonen, E. Vaananen, V.M. Kosma, N. Heisterkamp, J. Groffen, I. Mononen, Enzyme replacement therapy in a mouse model of aspartylglycosaminuria, FASEB J. 14 (2000) 361–367.
[12] H. Fu, M.P. Cataldi, T.A. Ware, K. Zaraspe, A.S. Meadows, D.A. Murrey, D.M. McCarty, Functional correction of neurological and somatic disorders at later stages of disease in MPS IIIA mice by systemic scAAV9-hSGSH gene delivery, Mol Ther Methods Clin Dev 3 (2016) 16036.
[13] B.L. Gliddon, J.J. Hopwood, Enzyme-replacement therapy from birth delays the development of behavior and learning problems in mucopolysaccharidosis type IIIA mice, Pediatr. Res. 56 (2004) 65–72.
[14] J.H. Grubb, C. Vogler, B. Levy, N. Galvin, Y. Tan, W.S. Sly, Chemically modified beta-glucuronidase crosses blood-brain barrier and clears neuronal storage in murine mucopolysaccharidosis VII, Proc. Natl. Acad. Sci. U. S. A. 105 (2008) 2616–2621.
[16] K.M. Hemsley, J.J. Hopwood, Delivery of recombinant proteins via the cerebrospinal fluid as a therapy option for neurodegenerative lysosomal storage diseases, Int. J. Clin. Pharmacol. Ther. 47 (Suppl. 1) (2009) S118–S123.
[17] K.M. Hemsley, J.J. Hopwood, Development of motor deficits in a murine model of mucopolysaccharidosis type IIIA (MPS-IIIA), Behav. Brain Res. 158 (2005) 191–199.
[18] R.J. Holley, S.R. Wood, B.W. Bigger, Delivering hematopoietic stem cell gene therapy treatments for neurological lysosomal diseases, ACS Chem. Neurosci. 10 (2019) 18–20.
[19] S.A. Jones, C. Breen, F. Heap, S. Rust, J. de Ruijter, E. Tump, J.P. Marchal, L. Pan, Y. Qiu, J.K. Chung, N. Nair, P.A. Haslett, A.J. Barbier, F.A. Wijburg, A phase 1/2 study of intrathecal heparan-N-sulfatase in patients with mucopolysaccharidosis IIIA, Mol. Genet. Metab. 118 (2016) 198–205.
[20] B. King, S. Hassiotis, T. Rozaklis, H. Beard, P.J. Trim, M.F. Snel, J.J. Hopwood, K.M. Hemsley, Low-dose, continuous enzyme replacement therapy ameliorates brain pathology in the neurodegenerative lysosomal disorder mucopolysaccharidosis type IIIA, J. Neurochem. 137 (2016) 409–422.
[23] B. King, P. Savas, M. Fuller, J. Hopwood, K. Hemsley, Validation of a heparan sulfate-derived disaccharide as a marker of accumulation in murine mucopolysaccharidosis type IIIA, Mol. Genet. Metab. 87 (2006) 107–112.
[24] A.A. Lau, A.C. Crawley, J.J. Hopwood, K.M. Hemsley, Open field locomotor activity and anxiety-related behaviors in mucopolysaccharidosis type IIIA mice, Behav. Brain Res. 191 (2008) 130–136.
[25] F. Maccari, N.C. Sorrentino, V. Mantovani, F. Galeotti, A. Fraldi, N. Volpi, Glycosaminoglycan levels and structure in a mucopolysaccharidosis IIIA mice and the effect of a highly secreted sulfamidase engineered to cross the blood-brain barrier, Metab. Brain Dis. 32 (2017) 203–210.
[26] Å. Makower, E. Arnelöf, T. Andersson, P.-O. Edlund, S. Gustavsson, S. Svensson Gelius, A. Tjernberg, Comparison of two LC-MS/MS methods for analysis of heparan sulfate levels in CSF and brain in a mouse model of MPS IIIA, Bioanalysis (2019) (Accepted manuscript).
[27] C. Martins, H. Hulkova, L. Dridi, V. Dormoy-Raclet, L. Grigoryeva, Y. Choi, A. Langford-Smith, F.L. Wilkinson, K. Ohmi, G. DiCristo, E. Hamel, J. Ausseil, D. Cheillan, A. Moreau, E. Svobodova, Z. Hajkova, M. Tesarova, H. Hansikova, B.W. Bigger, M. Hrebicek, A.V. Pshezhetsky, Neuroinflammation, mitochondrial defects and neurodegeneration in mucopolysaccharidosis III type C mouse model, Brain 138 (2015) 336–355.
[28] Y. Meng, I. Sohar, L. Wang, D.E. Sleat, P. Lobel, Systemic administration of tripeptidyl peptidase I in a mouse model of late infantile neuronal ceroid lipofuscinosis: effect of glycan modification, PLoS One 7 (2012) e40509.
[29] E.F. Neufeld, Enzyme replacement therapy - a brief history, in: A. Mehta, M. Beck, G. Sunder-Plassmann (Eds.), Fabry Disease: Perspectives from 5 Years of FOS (Oxford), 2006.
[30] K. Ohmi, D.S. Greenberg, K.S. Rajavel, S. Ryazantsev, H.H. Li, E.F. Neufeld, Activated microglia in cortex of mouse models of mucopolysaccharidoses I and IIIB, Proc. Natl. Acad. Sci. U. S. A. 100 (2003) 1902–1907.
[31] A. Oldfors, P. Sourander, Storage of lipofuscin in neurons in mucopolysaccharidosis. Report on a case of Sanfilippo's syndrome with histochemical and electron-microscopic findings, Acta Neuropathol. 54 (1981) 287–292.
[32] H. Parker, B.W. Bigger, The role of innate immunity in mucopolysaccharide diseases, J. Neurochem. 148 (5) (2019 Mar) 639–651, https://doi.org/10.1111/jnc.14632.
[33] V.A. Polito, S. Abbondante, R.S. Polishchuk, E. Nusco, R. Salvia, M.P. Cosma, Correction of CNS defects in the MPSII mouse model via systemic enzyme replacement therapy, Hum. Mol. Genet. 19 (2010) 4871–4885.
[34] T. Rozaklis, H. Beard, S. Hassiotis, A.R. Garcia, M. Tonini, A. Luck, J. Pan, J.C. Lamsa, J.J. Hopwood, K.M. Hemsley, Impact of high-dose, chemically modified sulfamidase on pathology in a murine model of MPS IIIA, Exp. Neurol. 230 (2011) 123–130.
[35] A. Ruzo, M. Garcia, A. Ribera, P. Villacampa, V. Haurigot, S. Marco, E. Ayuso, X.M. Anguela, C. Roca, J. Agudo, D. Ramos, J. Ruberte, F. Bosch, Liver production of sulfamidase reverses peripheral and ameliorates CNS pathology in mucopolysaccharidosis IIIA mice, Mol. Ther. 20 (2012) 254–266.
[36] S. Ryazantsev, W.H. Yu, H.Z. Zhao, E.F. Neufeld, K. Ohmi, Lysosomal accumulation of SCMAS (subunit c of mitochondrial ATP synthase) in neurons of the mouse model of mucopolysaccharidosis III B, Mol. Genet. Metab. 90 (2007) 393–401.
[38] A. Sergijenko, A. Langford-Smith, A.Y. Liao, C.E. Pickford, J. McDermott,

G. Nowinski, K.J. Langford-Smith, C.L. Merry, S.A. Jones, J.E. Wraith, R.F. Wynn, F.L. Wilkinson, B.W. Bigger, Myeloid/microglial driven autologous hematopoietic stem cell gene therapy corrects a neuronopathic lysosomal disease, Mol. Ther. 21 (2013) 1938–1949.

[40] N.C. Sorrentino, L. D'Orsi, I. Sambri, E. Nusco, C. Monaco, C. Spampanato, E. Polishchuk, P. Saccone, E. De Leonibus, A. Ballabio, A. Fraldi, A highly secreted sulphamidase engineered to cross the blood-brain barrier corrects brain lesions of mice with mucopolysaccharidoses type IIIA, EMBO Mol Med 5 (2013) 675–690.

[41] M. Tardieu, M. Zérah, M.L. Gougeon, J. Ausseil, S. de Bournonville, B. Husson, D. Zafeiriou, G. Parenti, P. Bourget, B. Poirier, V. Furlan, C. Artaud, T. Baugnon, T. Roujeau, R.G. Crystal, C. Meyer, K. Deiva, J.M. Heard, Intracerebral gene therapy in children with mucopolysaccharidosis type IIIB syndrome: an uncontrolled phase 1/2 clinical trial, Lancet Neurol. 16 (2017) 712–720.

[43] A. Urayama, J.H. Grubb, W.S. Sly, W.A. Banks, Mannose 6-phosphate receptor-mediated transport of sulfamidase across the blood-brain barrier in the newborn mouse, Mol. Ther. 16 (2008) 1261–1266.

[45] M.J. Valstar, G.J. Ruijter, O.P. van Diggelen, B.J. Poorthuis, F.A. Wijburg, Sanfilippo syndrome: a mini-review, J. Inherit. Metab. Dis. 31 (2008) 240–252.

[46] F.A. Wijburg, C.B. Whitley, J. Muenzer, S. Gasperini, M. Del Toro, N. Muschol, M. Cleary, C. Sevin, E. Shapiro, P. Bhargava, D. Kerr, D. Alexanderian, Intrathecal heparan-N-sulfatase in patients with Sanfilippo syndrome type a: a phase IIb randomized trial, Mol. Genet. Metab. 126 (2019) 121–130.

[47] F.L. Wilkinson, R.J. Holley, K.J. Langford-Smith, S. Badrinath, A. Liao, A. Langford-Smith, J.D. Cooper, S.A. Jones, J.E. Wraith, R.F. Wynn, C.L. Merry, B.W. Bigger, Neuropathology in mouse models of mucopolysaccharidosis type I, IIIA and IIIB, PLoS One 7 (2012) e35787.

[48] V. Haurigot, S. Marco, A. Ribera, M. Garcia, A. Ruzo, P. Villacampa, E. Ayuso, S. Anor, A. Andaluz, M. Pineda, G. Garcia-Fructuoso, M. Molas, L. Maggioni, S. Munoz, S. Motas, J. Ruberte, F. Mingozzi, M. Pumarola, F. Bosch, Whole body correction of mucopolysaccharidosis IIIA by intracerebrospinal fluid gene therapy, J. Clin. Invest. (2013).

[49] A. Ruzo, M. Garcia, A. Ribera, P. Villacampa, V. Haurigot, S. Marco, E. Ayuso, X.M. Anguela, C. Roca, J. Agudo, D. Ramos, J. Ruberte, F. Bosch, Liver production of sulfamidase reverses peripheral and ameliorates CNS pathology in mucopolysaccharidosis IIIA mice, Mol. Ther. 20 (2012) 254–266.

[50] F. Matthes, S. Stroobants, D. Gerlach, C. Wohlenberg, C. Wessig, J. Fogh, V. Gieselmann, M. Eckhardt, Efficacy of enzyme replacement therapy in an aggravated mouse model of metachromatic leukodystrophy declines with age, Hum. Mol. Genet. 21 (2015) 2599–2609.

[51] J.H. Dowson, H. Wilton-Cox, A. Oldfors, P. Sourander, Autofluorescence emission spectra of neuronal lipopigment in mucopolysaccharidosis (Sanfilippo's syndrome), Acta Neuropathol. 77 (1989) 426–429.

[52] A. Oldfors, P. Sourander, Storage of lipofuscin in neurons in mucopolysaccharidosis. Report on a case of Sanfilippo's syndrome with histochemical and electron-microscopic findings, Acta. Neuropathol. 54 (1981) 287–292.

[53] T. Rozaklis, H. Beard, S. Hassiotis, A.R. Garcia, M. Tonini, A. Luck, J. Pan, J.C. Lamsa, J.J. Hopwood, K.M. Hemsley, Impact of high-dose, chemically modified sulfamidase on pathology in a murine model of MPS IIIA, Exp. Neurol. 230 (2011) 123–130.

[54] C. Martins, H. Hulkova, L. Dridi, V. Dormoy-Raclet, L. Grigoryeva, Y. Choi, A. Langford-Smith, F.L. Wilkinson, K. Ohmi, G. DiCristo, E. Hamel, J. Ausseil, D. Cheillan, A. Moreau, E. Svobodova, Z. Hajkova, M. Tesarova, H. Hansikova, B.W. Bigger, M. Hrebicek, A.V. Pshezhetsky, Neuroinflammation, mitochondrial defects and neurodegeneration in mucopolysaccharidosis III type C mouse model, Brain 138 (2015) 336–355.